Journal Pre-proofs

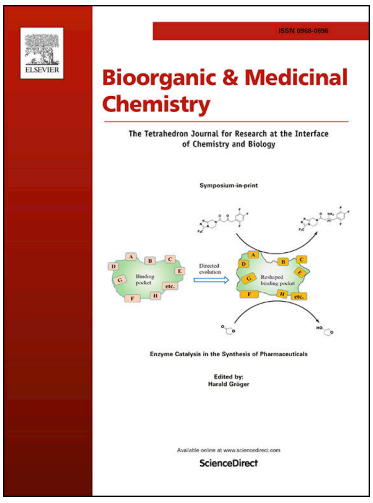

Design, synthesis, and anti-proliferative evaluation of new quinazolin-4(3*H*)-ones as potential VEGFR-2 inhibitors

Khaled. El-Adl, Abdel-Ghany A. El-Helby, Rezk R. Ayyad, Hazem A. Mahdy, Mohamed M. Khalifa, Hamdy A. Elnagar, Ahmed. B.M. Mehany, Ahmed. M. Metwaly, Mostafa. A. Elhendawy, Mohamed. M. Radwan, Mahmoud. A. ElSohly, Ibrahim. H. Eissa

PII: S0968-0896(20)30702-1
DOI: https://doi.org/10.1016/j.bmc.2020.115872
Reference: BMC 115872

To appear in: *Bioorganic & Medicinal Chemistry*

Received Date: 17 July 2020
Revised Date: 3 November 2020
Accepted Date: 6 November 2020

Please cite this article as: Khaled. El-Adl, A.A. El-Helby, R.R. Ayyad, H.A. Mahdy, M.M. Khalifa, H.A. Elnagar, A.B.M. Mehany, d.M. Metwaly, a.A. Elhendawy, d.M. Radwan, d.A. ElSohly, m.H. Eissa, Design, synthesis, and anti-proliferative evaluation of new quinazolin-4(3*H*)-ones as potential VEGFR-2 inhibitors, *Bioorganic & Medicinal Chemistry* (2020), doi: https://doi.org/10.1016/j.bmc.2020.115872

Design, synthesis, and anti-proliferative evaluation of new quinazolin-4(3*H*)-ones as potential VEGFR-2 inhibitors

Khaled. El-Adl[a,b,*], Abdel-Ghany A. El-Helby[a] , Rezk R. Ayyad[a], Hazem A. Mahdy[a], Mohamed M. Khalifa[a], Hamdy A. Elnagar[a], Ahmed. B. M. Mehany[c], Ahmed. M. Metwaly[d], Mostafa. A. Elhendawy[e,f], Mohamed. M. Radwan[f, g], Mahmoud. A. ElSohly*[f,h], Ibrahim. H. Eissa*[a]

[a] Pharmaceutical Medicinal Chemistry & Drug Design Department, Faculty of Pharmacy (Boys), Al-Azhar University, Cairo11884, Egypt.

[b] Pharmaceutical Chemistry Department, Faculty of Pharmacy, Heliopolis University for Sustainable Development, Cairo, Egypt.

[c] Zoology Department, Faculty of Science, Al-Azhar University, Cairo 11884, Egypt.

[d] Pharmacognosy Department, Faculty of Pharmacy (Boys), Al-Azhar University, Cairo 11884, Egypt.

[e] Department of Agriculture Chemistry, Faculty of Agriculture, Damietta University, Damietta, Egypt

[f] National Center for Natural Products Research, University of Mississippi, MS 38677, USA.

[g] Department of Pharmacognosy, Faculty of Pharmacy, Alexandria University, Alexandria, Egypt.

[h] Department of Pharmaceutics and Drug Delivery, University of Mississippi, University, MS 38677, USA.

*** Corresponding authors:**

Ibrahim H. Eissa

Pharmaceutical Medicinal Chemistry & Drug Design Department, Faculty of Pharmacy (Boys), Al-Azhar University, Cairo 11884, Egypt**.**

Email: Ibrahimeissa@azhar.edu.eg

Khaled. El-Adl

Pharmaceutical Medicinal Chemistry & Drug Design Department, Faculty of Pharmacy (Boys), Al-Azhar University, Cairo 11884, Egypt**.**

Email: eladlkhaled74@yahoo.com

Abstract

Inhibiting VEGFR-2 has been set up as a therapeutic strategy for treatment of cancer. Thus, nineteen new quinazoline-4(3*H*)-one derivatives were designed and synthesized. Preliminary cytotoxicity studies of the synthesized compounds were evaluated against three human cancer cell lines (HepG-2, MCF-7 and HCT-116) using MTT assay method. Doxorubicin and sorafenib were used as positive controls. Five compounds were found to have promising cytotoxic activities against all cell lines. Compound **16$_f$**, containing a 2-chloro-5-nitrophenyl group, has emerged as the most active member. It was approximately 4.39-, 5.73- and 1.96-fold more active than doxorubicin and 3.88-, 5.59- and 1.84-fold more active than sorafenib against HepG2, HCT-116 and MCF-7 cells, respectively. The most active cytotoxic agents were further evaluated *in vitro* for their VEGFR-2 inhibitory activities. The results of *in vitro* VEGFR-2 inhibition were consistent with that of the cytotoxicity data. Molecular docking of these compounds into the kinase domain, moreover, supported the results.

Keywords: Anticancer; Molecular docking; quinazolin-4(3*H*)-one; VEGFR-2.

1. Introduction

Tumor angiogenesis plays a vital role in cancer cell survival, tumor growth and the development of distant metastasis [1-3]. Pathological angiogenesis has been associated with a diversity of diseases, including diabetes retinopathy, psoriasis, rheumatoid arthritis and cancer [4]. Numerous regulators of angiogenesis have been recognized and characterized [5, 6]. Among them Vascular endothelial growth factor (VEGF) is considered as a key angiogenic factor [7].

VEGF is secreted by tumors [8]. It induces a mitogenic response via its binding to one of three tyrosine kinase receptors (VEGFR-1–3) on the nearby endothelial cells [8]. Overexpression of VEGF have been noticed in several types of cancer including colorectal cancer [11], breast cancer [12] and hepatocellular carcinoma [13]. Accordingly, inhibition of this signaling pathway should block angiogenesis and subsequent tumor growth [9, 10]. There is much evidence that direct inhibition of the kinase activity of VEGFR-2 (also referred to as the kinase insert domain containing receptor (KDR)) will result in the reduction of angiogenesis and the suppression of tumor growth [11].

Recently, a lot of researches are focusing on the development of novel VEGFR-2 inhibitors [12]. Many VEGFR-2 inhibitors have been reported with significant potency to inhibit tumor angiogenesis (**Fig. 1, 2**) [13]. Several small molecule VEGFR-2 inhibitors, such as the birdlore derivative sorafenib **1** (BAY-43-9006, Bayer) [14], the indol-2-one derivative sunitinib **2** (SU-11248, Pfizer) [14], and quinolone derivative tivozanib **3** (FOTIVDA, Eusa Pharma UK) [15] have been clinically approved for the treatment of several cancer diseases.

Numerous small VEGFR-2 inhibitors molecules have progressed to the clinical evaluation stage [16]. Linifanib **4** (ABT-869, Abbott) is a novel, orally active VEGFR-2 inhibitor that exhibits significant antitumor and antiangiogenic activities and is currently in phase III trials [13, 17]. Cediranib **5** (AZD2171, AstraZeneca) is an orally active angiogenesis inhibitor that works by selectively inhibiting the tyrosine kinase activity of all VEGF receptor subtypes [18]. Cediranib **5**, a quinazoline derivative, is being tested in phase III clinical trials for treatment of ovarian cancer [19]. However, the development of novel VEGFR-2 inhibitors analogs displayed a field of great interest, as demonstrated by the number of patents filed and of a lot of papers published in the last years [10].

VEGFR-2 was reported to be substantially upregulated in HepG-2 cells in a dose-dependent manner with the stimulation of the hepatocyte growth factor (HGF), which is involved in cell proliferation, invasion, and angiogenesis of hepatocellular carcinoma (HCC) [20-22]. Blockade of VEGFR-2 signaling revealed a marked inhibition on both the growth and metastasis of HCC [22,

23]. As well, VEGFR-2 was found to be crucial to cell survival and regulates endothelial differentiation in both the breast cancer cells (MCF-7) [23] and human colorectal carcinoma (HCT-116) [24, 25]. Over-expression of VEGFR-2 receptors in breast cancer cells has documented a contributor in resistance of such cancer type to the chemotherapeutic effect of tamoxifen [26]. VEGFR-2 degraders were documented to impair the *in vitro* endothelial differentiation, and to promote angiogenesis, suggesting a VEGFR-2-mediated mechanism of antiproliferative activity in human colorectal carcinoma [24].

Quinazolin-4(3*H*)-one is a promising class of heterocycles that is well-tolerated in humans [27] and possesses antitumor activity [28-30]. Moreover, it is the backbone of many bioactive compounds that show potential activities as VEGFR inhibitors [4, 31]. In addition, several new sulfonamide [29] and thiosemicarbazone [32] moieties were reported to possess antitumor activities.

In view of this, our rationale of molecular design aimed to develop small quinazolin-4(3*H*)-ones in order to act as VEGFR-2 inhibitors. They displayed potent antiproliferative effects and could be considered as promising lead compounds for further optimization. A molecular docking model and preliminary SAR based on enzymatic inhibitory activity were also discussed.

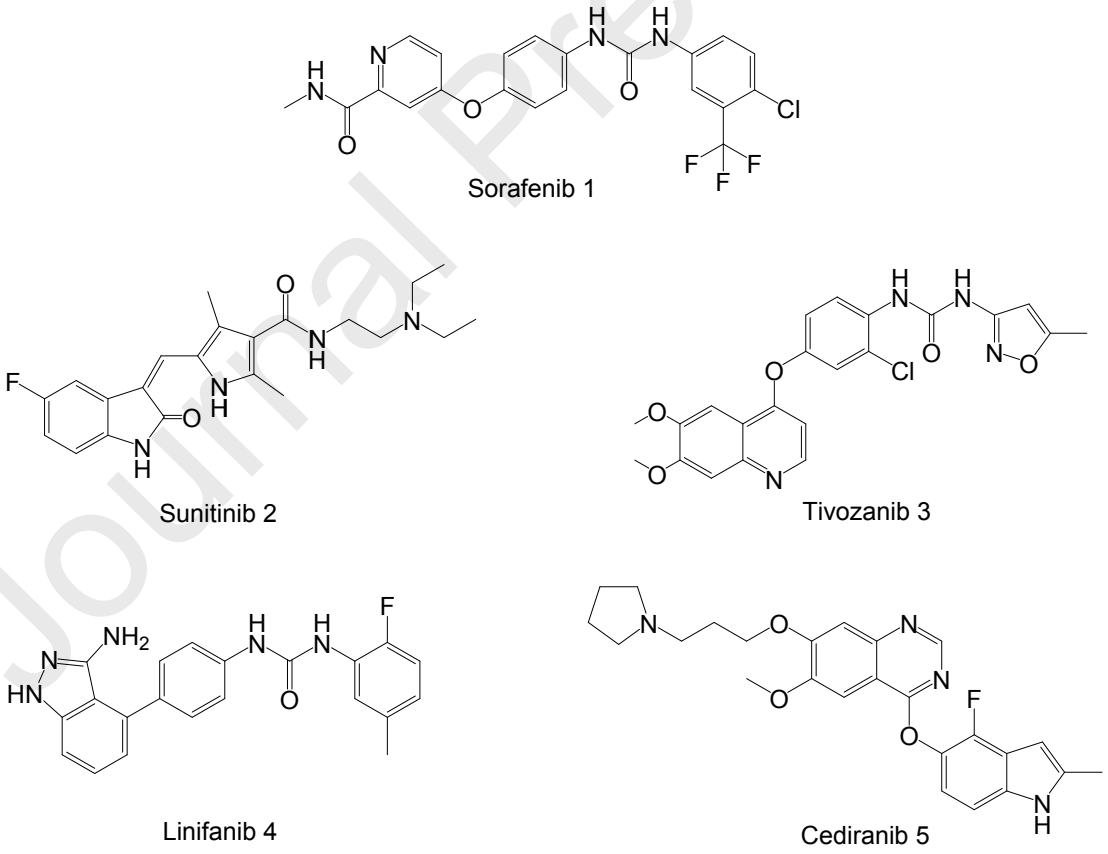

Fig. 1. Chemical structures of VEGFR-2 inhibitors

1.1. Rational of molecular design

In continuation of our previous works that proved potential anticancer activities of novel chemical agents [33-46], herein we present the synthesis and the biological evaluation of some novel derivatives carrying modifications in the quinazoline-4(3*H*)-one scaffolds.

Analyzing the binding interactions of sorafenib **1** and different VEGFR-2 inhibitors and the common pharmacophoric features shared by them [47-49] revealed that VEGFR-2 inhibitors, though being highly diverse in structure, share four common feature pharmacophores for binding as illustrated in **Fig. 2** and **Fig. 3**. (**i**) A flat aromatic ring system (the left cyan color) of the main scaffold that adopts the active site via formation of an essential hydrogen bond with the backbone NH of Cys917 residue, the key amino acid residue in the catalytic ATP-binding domain [48]. And therefore, this flat system should contain at least one H-bond acceptor (N atom is preferred, followed by the O atom). (**ii**) A central aryl ring or spacer (presented by the brown color), occupying the linker region between the ATP-binding domain and the DFG domain of the enzyme [50]. (**iii**) A functional group (presented by the yellow color) acting as pharmacophore (e.g., amide or urea) that forming two hydrogen bonds with the enzyme allosteric site residues: one hydrogen bond with the side chain of a conserved glutamic acid in the C-helix (Glu 883) and the other with the backbone amide of aspartic acid in the DFG motif (Asp 1044) [51]. (**iv**) All VEGFR-2 inhibitors also have a hydrophobic moiety (the right pink color) that is located just after the hydrogen bond donor–acceptor pair forming van der Waals interactions with the allosteric site [52, 53].

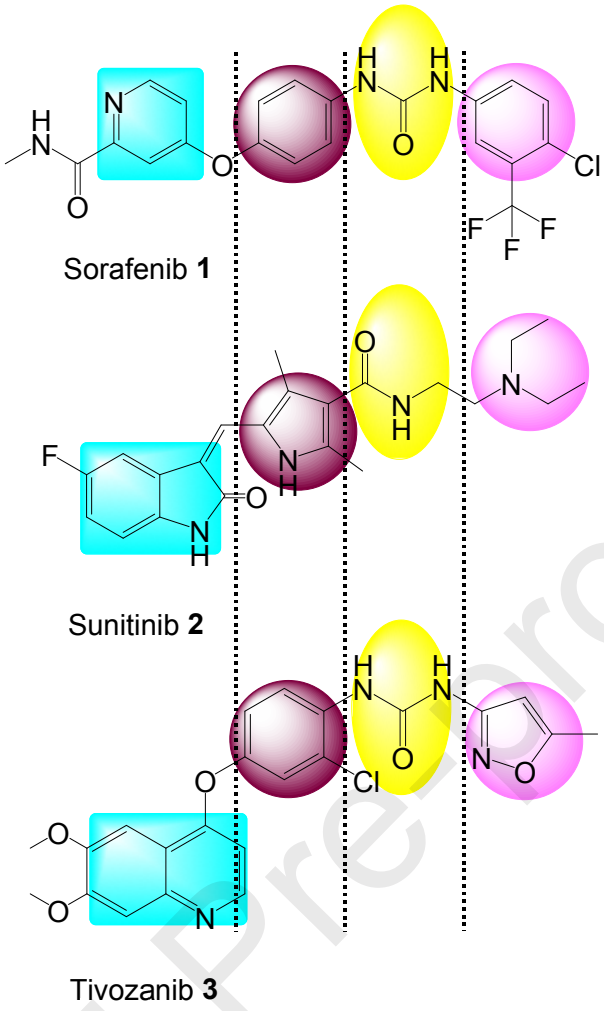

Fig. 2. Basic pharmacophoric features of VEGFR-2 inhibitors

Our design was based on targeting VEGFR-2 in its DFG-out conformation. Inspection of known type-II inhibitors, especially sorafenib, revealed that the conserved hydrogen bonds between the ligand and the allosteric site residues were done using urea or amide moieties. In this respect, we designed novel compounds based on quinazoline core molecularly hybridized with effective antitumor moieties containing urea, amide and sulfonamide pharmacophores with extended alkyl or aryl groups. The main core of our molecular design comprised bio-isosteric modification approaches of VEGFR-2 inhibitors at four different positions (**Fig. 3)**.

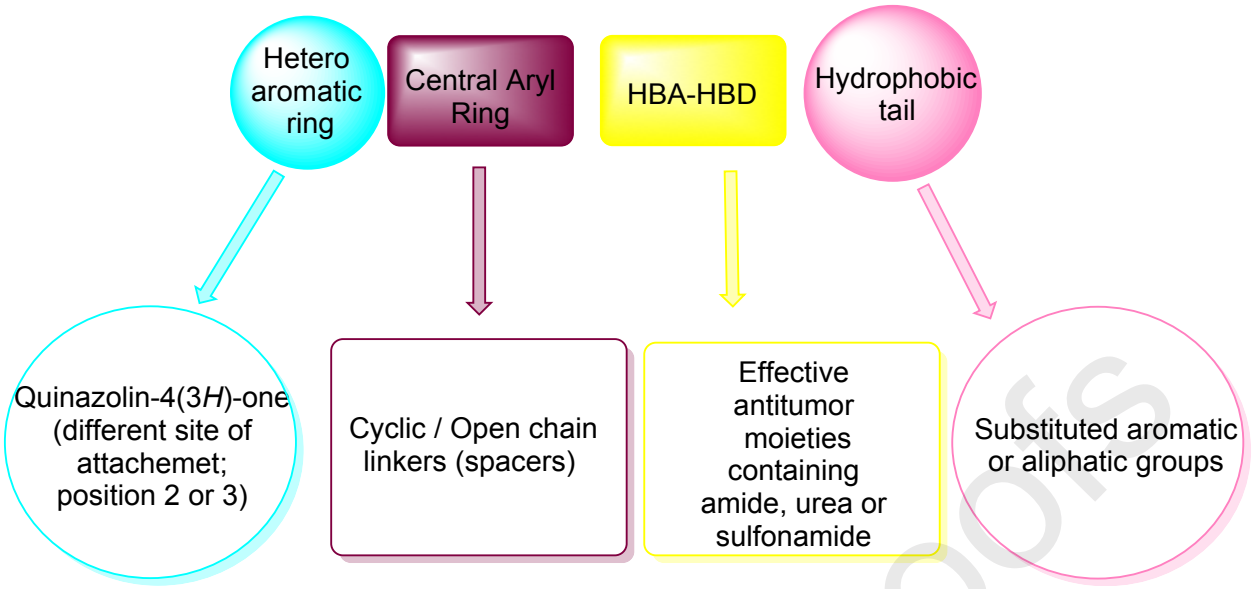

Fig. 3. Summary for the possible modifications of VEGFR-2 inhibitors

The first position was the heterocyclic aromatic ring in which the 2-mercapto-3-(4-methylphenyl)quinazolin-4(3*H*)-one moiety was used. The choice of this quinazoline moiety was based on some bio-isoeteric considerations, **i**) the bicyclic structure of quinazoline core is convenient to the large size space of the ATP binding region [53], **ii**) the heterocyclic nitrogen atoms serve as hydrogen-bond acceptors conferring excellent VEGFR-2 potency.

The second position was the linker (spacer) region. The length of the linker was modified to be four atom bridges in addition to a phenyl moiety. The third position was the HBA/HBD region (pharmacophore). We used many different effective anticancer moieties comprises the essential HBA/HBD features to play the role of the pharmacophore. The pharmacophores were designed to be open forms. The used open chain pharmacophores were hydrazone, sulfonamide, acetamidobenzamide, 2-hydroxybenzolhydrazine, and thiosemicarbazone moieties.

Finally, the terminal hydrophobic moieties were selected to be aromatic heterocyclic, aromatic non-heterocyclic or aliphatic structures. The wide variety of modifications enabled us to study the SAR of these compounds as effective anti-cancer agents with potential VEGFR-2 inhibitory activities which is considered as a crucial objective of our work. All modification pathways and molecular design rationale were demonstrated and summarized in **Fig 4**.

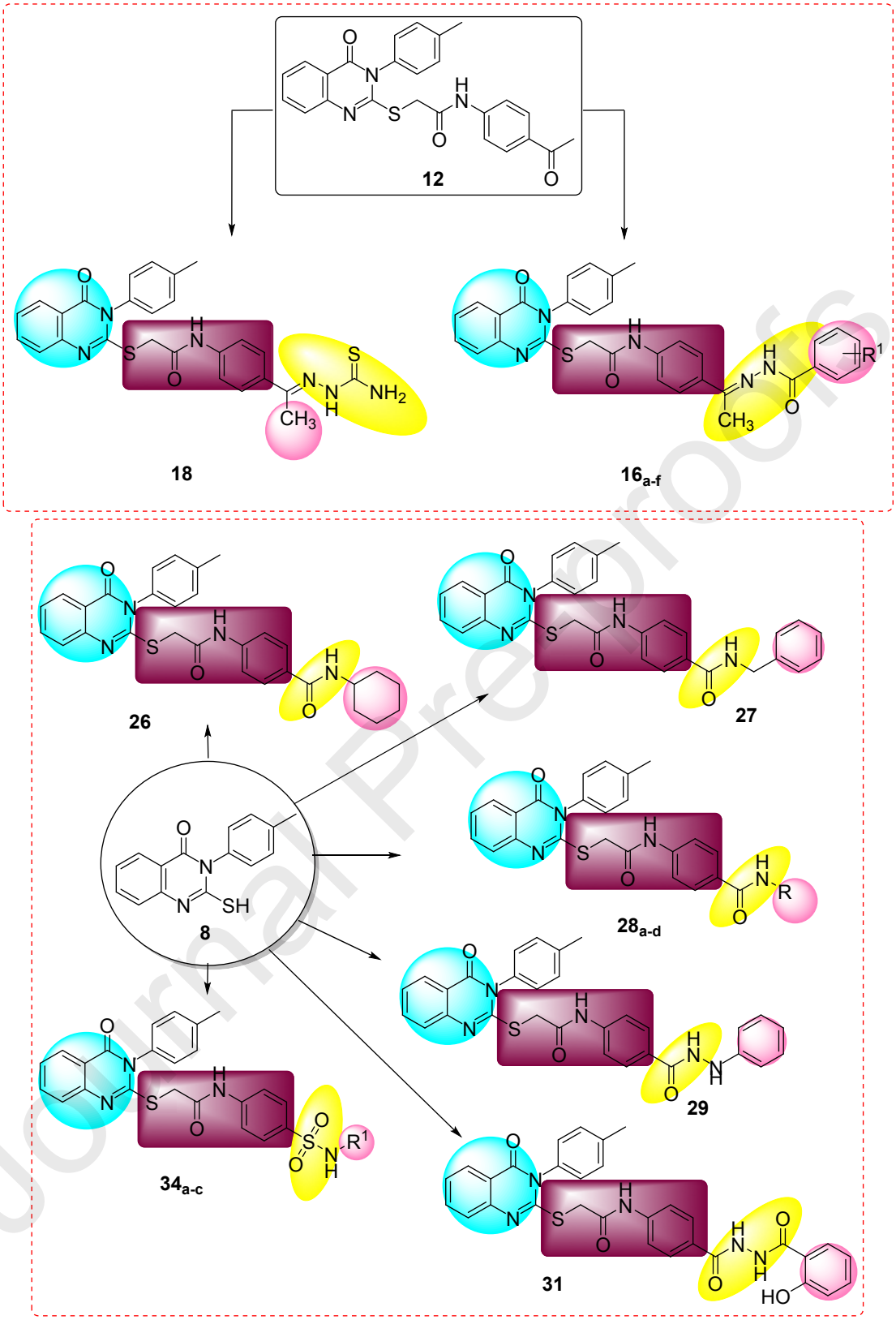

Fig. 4. Design of the newly proposed quinazolinone derivatives as VEGFR-2 inhibitors.

2. Results and discussion

2.1. Chemistry

In our research to discover new anticancer compounds, we designed and evaluated pharmacologically nineteen quinazolinone derivatives as potent VEGFR-2 inhibitors. These compounds were prepared via a generalized route outlined in **Schemes 1-6**.

The commercial available anthranilic acid **6** was primary reacted in alkaline media with *p*-toluidine **7** in the presence of carbon disulfide to furnish 2-mercapto-3-(4-methylphenyl)quinazolin-4(3*H*)-one **8** [54] which was then heated with alcoholic potassium hydroxide to afford the corresponding potassium salt **9** as the reported procedure [55]. On the other side, 4-aminoacetophenone **10** was stirred with chloroacetyl chloride in dry DMF at room temperature to produce *N*-(4-acetylphenyl)-2-chloroacetamide **11** [56]**.** The previously prepared potassium salt **9** was refluxed, however, with compound **11** according to the method reported by El-Helby *et. al*. to afford compound **12** (**Scheme 1**) [57].

IR spectrum of compound **12** confirmed the presence of carbonyl absorption bands at 1670, 1685 and 1700 cm^{-1} and NH band at 3234 cm^{-1}. Its ^1H NMR spectra showed singlet signals of the aliphatic protons at δ 2.55 and 4.11 ppm in addition to another one at δ 2.42 corresponding to $COCH_3$, SCH_2 and Ar-CH_3 protons, respectively (**Scheme 1**).

Scheme 2 was initiated via synthesis of some benzoic acid hydrazide intermediates $\mathbf{15_{a-f}}$. These intermediates were prepared by esterification of (un)substituted benzoic acids $\mathbf{13_{a-f}}$ with absolute ethanol in the presence of sulfuric acid as a catalyst [58] followed by refluxing with hydrazine hydrate [59, 60]. The later intermediates were allowed to react with compound **12** in the presence of a catalytic amount of glacial acetic acid to give the target compounds $\mathbf{16_{a-f}}$ [61]**.** The formation of compounds $\mathbf{16_{a-f}}$ were confirmed by ^1H NMR spectra which showed shifting of the CH_3 protons to a range of δ 2.41-2.43 ppm than the CH_3 protons of the corresponding ketone derivative **12**. Moreover, D_2O exchangeable singlet signals appeared at a range of δ 10.74-11.33 ppm that corresponds to the NH protons.

Similarly, compound **12** was treated with thiosemicarbazide **17** to afford the corresponding derivative **18** [61] which was approved by its spectral data (**Scheme 2**).

Scheme 3 was started primarily with stirring of 4-aminobenzoic acid **19** with chloroacetyl chloride in DMF at room temperature to give 4-(3-chloroacetamido) benzoic acid **20** [62].

Different carboxylic acid amide intermediates were prepared from 4-(3-chloroacetamido) benzoic acid **20** following the mixed anhydride procedure. This procedure involves the activation of the acid as a mixed carboxylic-carbonic acid anhydride [63, 64]. The anhydride **21** was generated by the action of ethyl chloroformate in the presence of TEA, and is not isolated before the

subsequent reaction. The formed anhydride was then treated with different aromatic or aliphatic amines at room temperature to give the desired intermediates **22, 23, 24$_{a-d}$** and **25** (**Scheme 3**).

With respect to the previously prepared intermediates, they were allowed to interact with the potassium salt **9** in DMF affording compounds **26, 27, 28$_{a-d}$** and **29 (Scheme 4)** [65]**. IR** spectra of this series confirmed presence of the carbonyl absorption band at a range of 1654-1751 cm^{-1} and presence of NH band at a range of 3179 - 3462 cm^{-1}. ^{1}H NMR spectra showed singlet signals of the aliphatic -SCH_2 protons at a δ range of 4.09 - 4.15 ppm and presence of D_2O exchangeable NH-amide protons at a δ range of 8.32- 10.74 ppm.

The potassium salt **9** reacted also with compound **30**, prepared by mixed anhydride procedure via the reaction of 4-(2-chloroacetamido) benzoic acid **20** with 2-hydroxybenzohydrazide **15$_e$**, to give the target compound **31** (**Scheme 5**) [64]. The formation of compound **31** was confirmed by ^{1}H NMR spectra which showed the appearance of a singlet signal of the aliphatic -SCH_2 protons at δ 4.12 ppm in addition to D_2O exchangeable signals of the NH-amide protons at δ 10.47 and 10.68 ppm.

The intermediates **33$_{a-c}$** were prepared according to the reported methods [66, 67]. These intermediates were used in the present work to introduce the *N*-(4-(*N*-(substituted)sulfamoylphenyl)acetamide moieties to the previously prepared potassium salt **9** to afford compounds **34$_{a-c}$** (**Scheme 6**) [65]. IR spectra of this series confirmed the presence of the carbonyl absorption bands at a range of 1710-1671cm^{-1} and NH bands at a range of 3447-3117 cm^{-1}. ^{1}H NMR spectra showed singlet signals of the aliphatic -SCH_2 protons at a δ range of 4.09 - 4.12 ppm and D_2O exchangeable NH-amide protons at a δ range of 9.67-10.90 ppm.

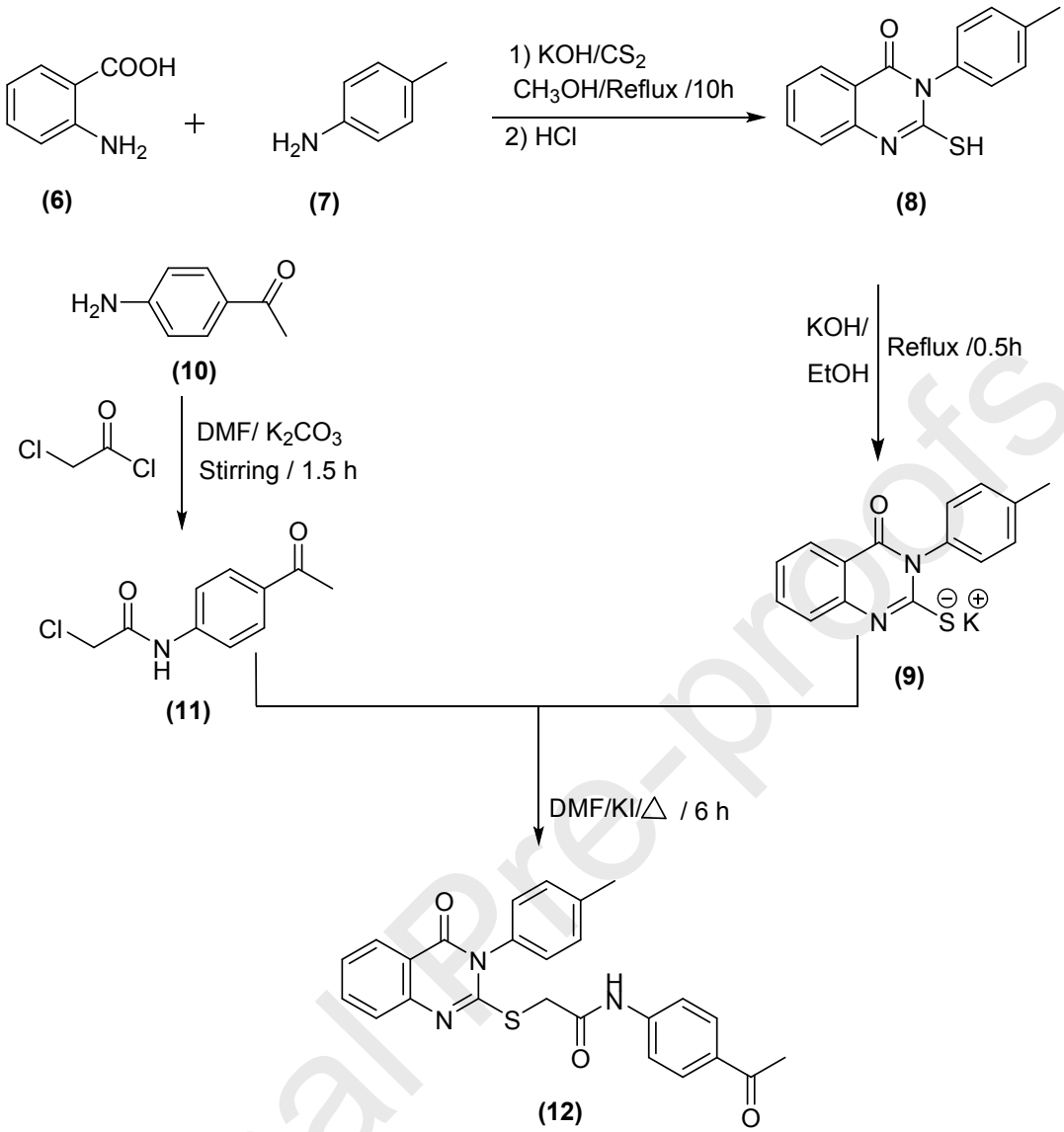

Scheme 1. General procedure for synthesis of target compound 12.

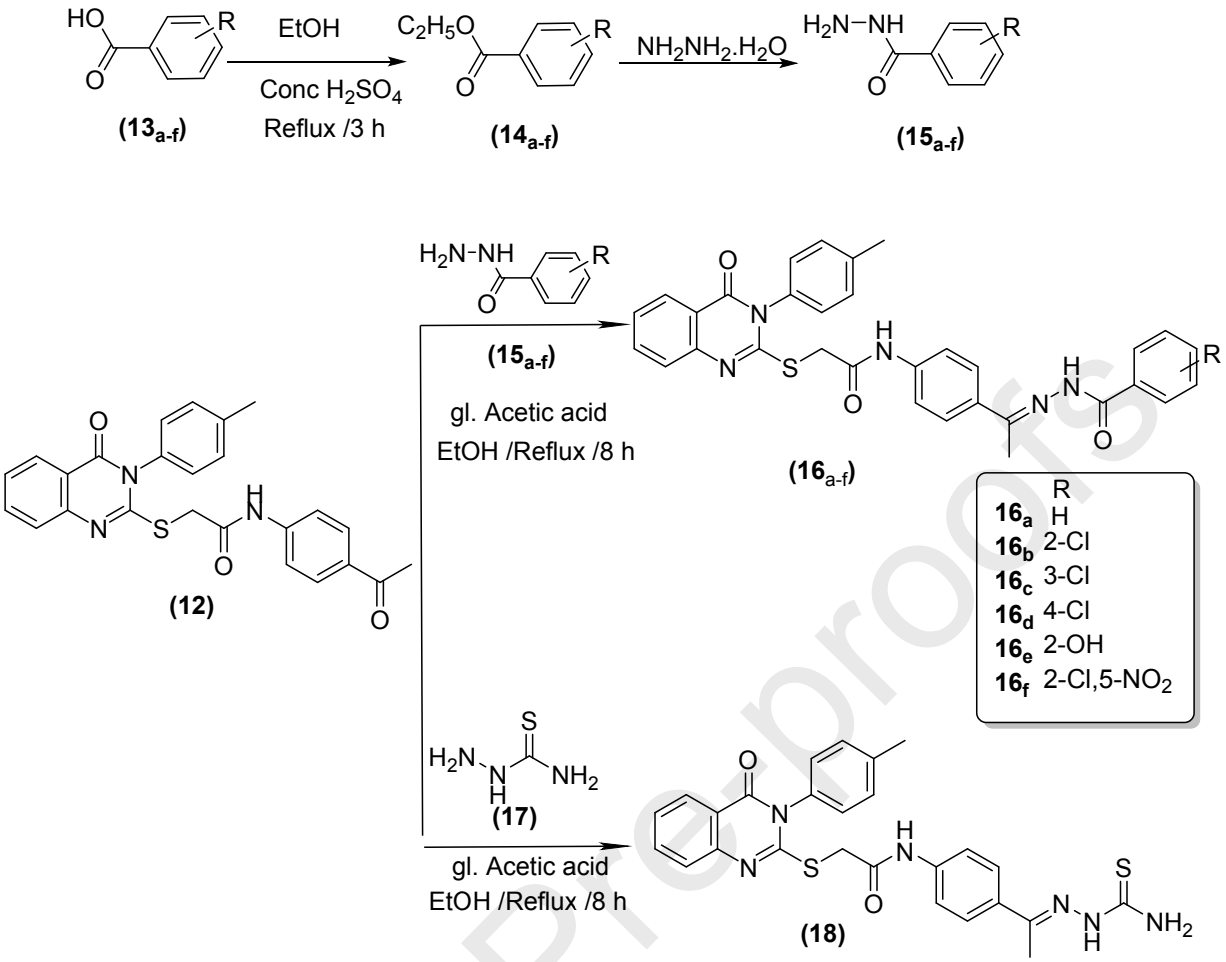

Scheme 2. General procedure for synthesis of target compounds $\mathbf{16_{a-f}}$ and **18**.

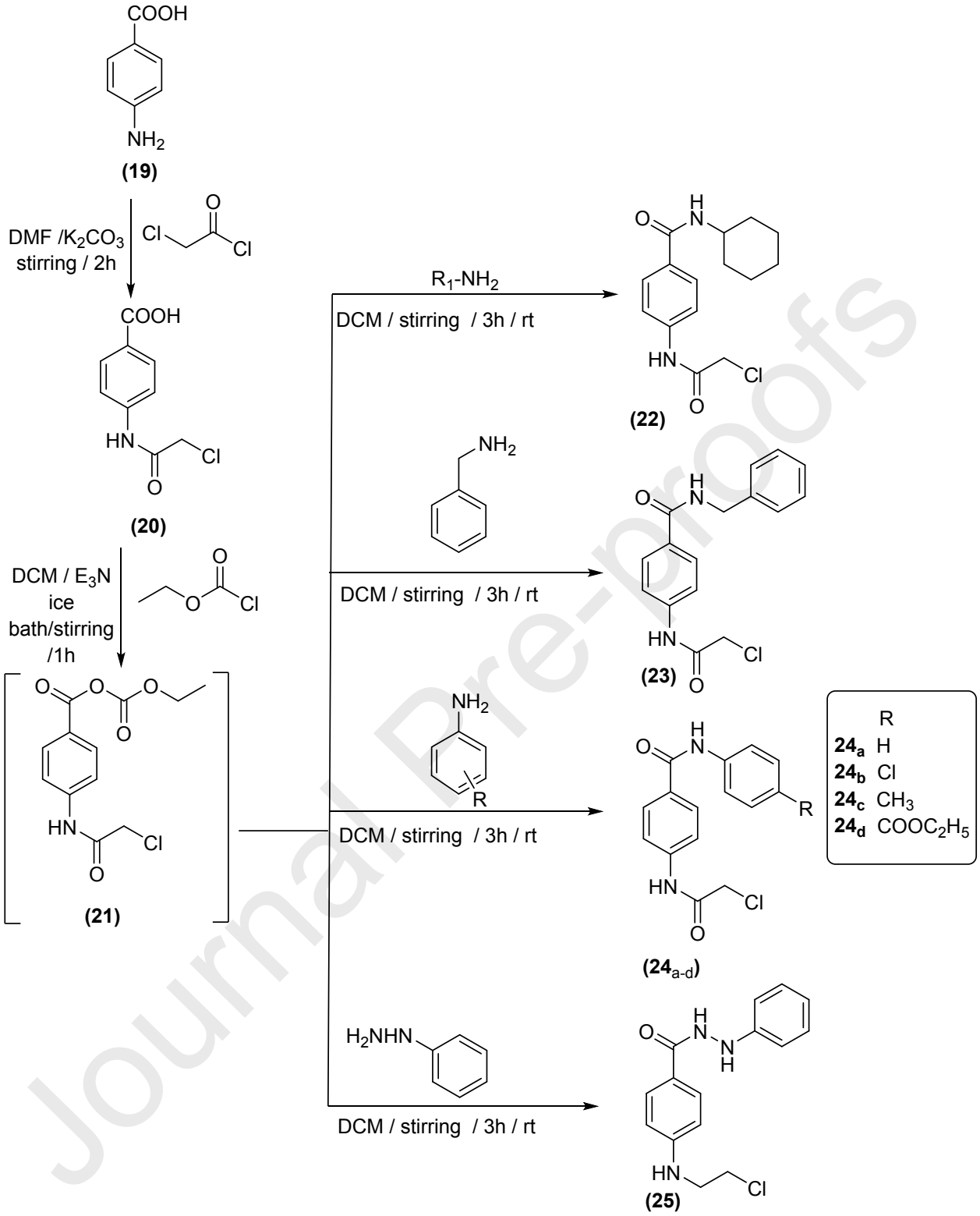

Scheme 3. General procedure for synthesis of the intermediates **22, 23, 24$_{a-d}$** and **25.**

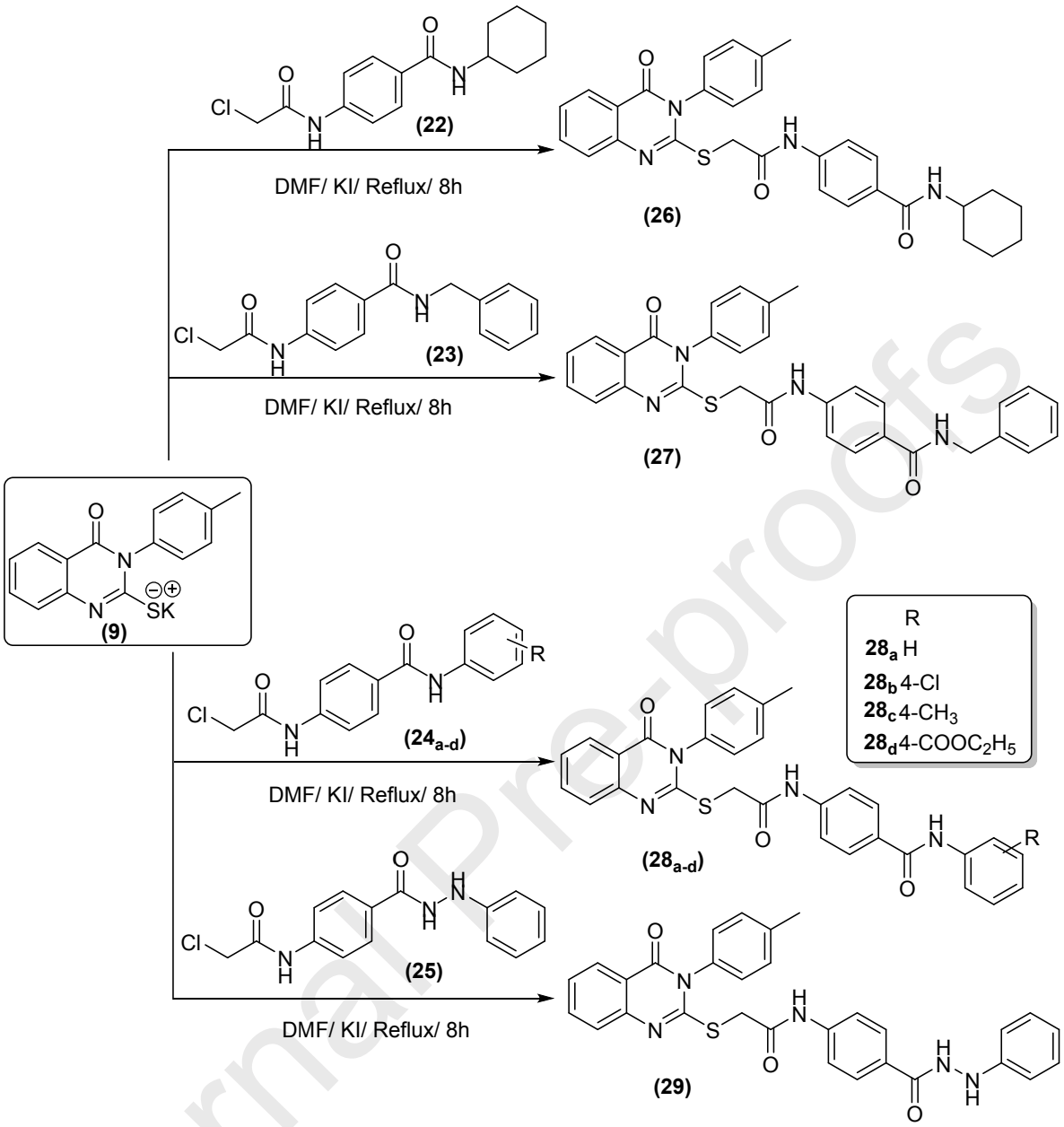

Scheme 4. General procedure for synthesis of target compounds **26, 27, 28**$_{a-d}$ and **29.**

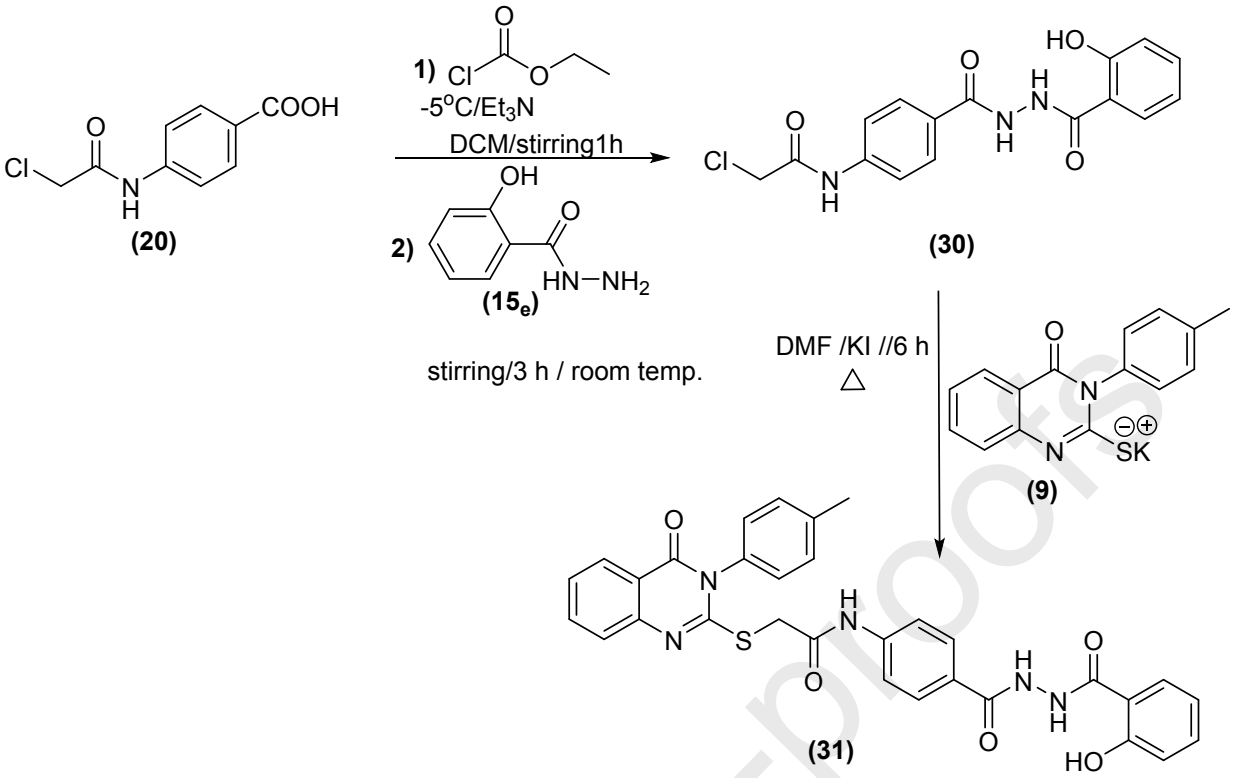

Scheme 5. General procedure for synthesis of target compound **31.**

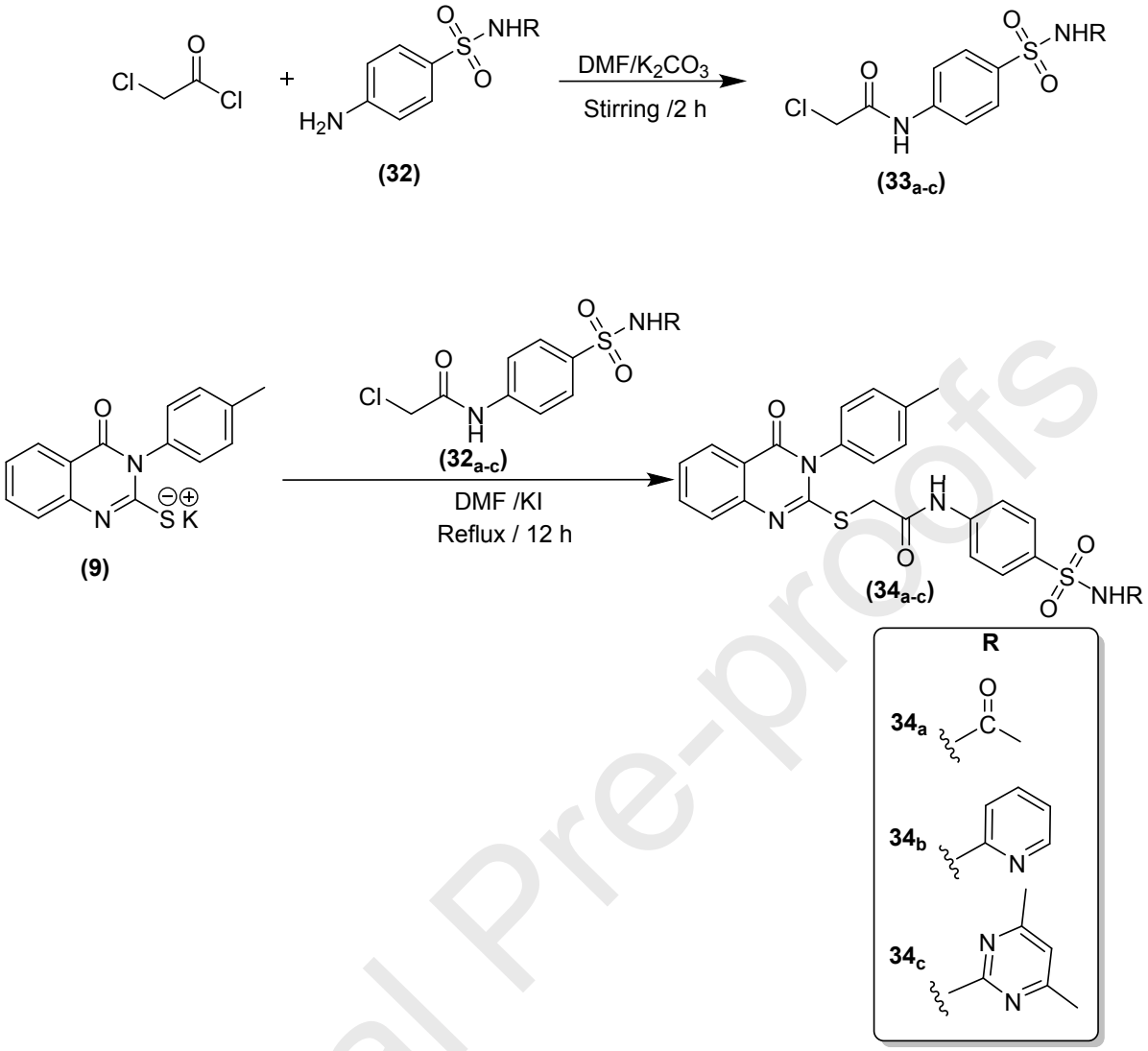

Scheme 6. General procedure for synthesis of target compounds **34$_{a-c}$.**

2.2. Biological evaluation

2.2.1. *In vitro* anti-proliferative activity

The synthesized quinazolin-4(3*H*)-one derivatives were evaluated for their *in vitro* anti-proliferative effects against a panel of three human tumor cell lines namely; hepatocellular carcinoma (HepG-2), colorectal carcinoma (HCT-116) and breast cancer (MCF-7). In such cell lines, VEGF has been overexpressed [68-70]. Sorafenib and doxorubicin, two of the most effective anti-proliferative drugs, were used as standard drugs. The inhibitory effects on cell proliferation were determined by MTT assay [71-73] and the results were expressed as growth inhibitory concentration (IC_{50}) values and summarized in **Table 1**.

From the obtained results, it was obvious that the tested compounds displayed excellent, marked, moderate or weak anti-proliferative activities against the three

tested cell lines with a clear observation that almost all the tested compounds showed better activities against HepG-2 and HCT-116 than against MCF-7.

In general, compounds **16$_f$**, **18**, **28$_b$, 34$_a$** and **34$_c$** were found to be the most potent derivatives. However, they were found to be mostly more active than the standard and sometimes a little lower or almost the same. In particular, compound **16$_f$** (IC_{50} = 1.88 ± 0.07, 1.68 ± 0.06 and 3.91 ± 0.15 µM) was found to be the most potent counterpart as it was 4.39, 5.73 and 1.96 times more active than doxorubicin (IC_{50} = 8.28 ± 0.33, 9.63 ± 0.38 and 7.67 ± 0.30 µM) and 3.88, 5.59 and 1.84 times more active than sorafenib (IC_{50} = 7.31 ± 0.29, 9.40 ± 0.37and 7.21 ± 0.28 µM) against HepG2, HCT-116 and MCF-7 cells, respectively. In addition, compound **28$_b$** possessed excellent anti-proliferative activities against the three cell lines; however, its IC_{50} values against HepG2, HCT-116 and MCF-7 were 4.12 ± 0.12, 3.67 ± 0.14 and 5.99 ± 0.23 µM, respectively.

On the other hand, the rest of compounds exhibited mild to moderate activity according to the type of cancer cell line with IC_{50} ranging from 8.27 ± 0.33 to 43.96 ± 1.75 µM.

Table 1. Anti-proliferative activities of the tested compounds toward HepG-2, HCT-116 and MCF-7 cell lines

Comp.	***In vitro* anti-proliferative IC_{50} (µM)[a]**					
	HepG-2	***Adjusted P Value[b]***	**HCT-116**	***Adjusted P Value[b]***	**MCF-7**	***Adjusted P Value[b]***
12	12.33 ± 0.49	<0.0001	8.27 ± 0.33	0.3784	13.48 ± 0.53	<0.0001
16$_a$	30.49 ± 1.21	<0.0001	28.98 ± 1.15	<0.0001	35.92 ± 1.43	<0.0001
16$_b$	22.56 ± 0.90	<0.0001	17.06 ± 0.68	<0.0001	23.04 ± 0.92	<0.0001
16$_c$	33.81 ± 1.35	<0.0001	30.41 ± 1.21	<0.0001	40.86 ± 1.63	<0.0001
16$_d$	41.55 ± 1.66	<0.0001	37.14 ± 1.48	<0.0001	43.96 ± 1.75	<0.0001
16$_e$	11.92 ± 0.47	<0.0001	12.37 ± 0.49	<0.0001	15.44 ± 0.61	<0.0001
16$_f$	1.88 ± 0.07	<0.0001	1.68 ± 0.06	<0.0001	3.91 ± 0.15	0.0009
18	8.38 ± 0.33	0.6308	8.32 ± 0.33	0.4363	9.89 ± 0.39	0.0101
26	16.48 ± 0.65	<0.0001	14.08 ± 0.56	<0.0001	24.89 ± 0.99	<0.0001
27	17.43 ± 0.69	<0.0001	13.42 ± 0.53	<0.0001	18.31 ± 0.73	<0.0001
28$_a$	21.76 ± 0.87	<0.0001	16.55 ± 0.66	<0.0001	26.85 ± 1.07	<0.0001
28$_b$	4.12 ± 0.12	0.0002	3.67 ± 0.14	<0.0001	5.99 ± 0.23	0.6504

28_c	19.02 ± 0.76	<0.0001	17.43 ± 0.69	<0.0001	28.35 ± 1.13	<0.0001
28_d	21.51 ± 0.86	<0.0001	17.02 ± 0.68	<0.0001	23.74 ± 0.94	<0.0001
29	12.14 ± 0.48	<0.0001	9.40 ± 0.37	>0.9999	16.07 ± 0.64	<0.0001
31	11.69 ± 0.46	<0.0001	10.76 ± 0.43	0.1773	14.38 ± 0.57	<0.0001
34_a	4.19 ± 0.16	0.0003	6.14 ± 0.24	<0.0001	6.79 ± 0.27	0.9992
34_b	29.98 ± 1.19	<0.0001	24.11 ± 0.96	<0.0001	30.64 ± 1.22	<0.0001
34_c	6.76 ± 0.27	0.9912	5.24 ± 0.20	<0.0001	7.10 ± 0.28	0.9998
Doxorubicin	8.28 ± 0.33	0.7475	9.63 ± 0.38	0.9994	7.67 ± 0.30	0.9991
Sorafenib	7.31 ± 0.29		9.40 ± 0.37		7.21 ± 0.28	

[a] All experiments were repeated three times. The results were expressed as the mean ± standard deviation (mean ± SD) calculated from three independent experiments (n = 3). P value < 0.05 was considered significant.

[b] Adjusted ***P*** Value compared to standard sorafenib

2.2.2. *In vitro* VEGFR-2 enzyme assay inhibition

The most active cytotoxic compounds (**12**, **16_e**, **16_f**, **18**, **27**, **28_a**, **28_b**, **29**, **31**, **34_a** and **34_c**) were further assessed to determine their inhibitory activities against VEGFR-2 with sorafenib as positive control. The results were summarized in **Table 2**. As shown in **Table 2**, the majority of the tested compounds displayed superior to moderate enzyme inhibitory activity with IC_{50} values ranging from 0.290 ± 0.05 to 0.790 ± 0.11 µg/mL. Among them, five compounds, **16_f, 18, 28_b, 34_a** and **34_c**, out of eleven potently inhibited VEGFR-2 with IC_{50} values (0.290 ± 0.05, 0.517 ± 0.07, 0.380 ± 0.04, 0.377 ± 0.04, and 0.415 ± 0.03 µg/mL, respectively) than the reference drug; Sorafinib (0.588 µg/mL).

Table 2: IC_{50} values of the tested compounds against VEGFR-2

Comp.	VEGFR-2 inhibition IC_{50} (µg/mL)[a]
12	0.790 ± 0.11
18	0.517 ± 0.07
16_e	0.610 ± 0.09
16_f	0.290 ± 0.05
27	0.751 ± 0.10
28_a	0.713 ± 0.07
28_b	0.380 ± 0.04
29	0.648 ± 0.06
31	0.619 ± 0.05
34_a	0.377 ± 0.04
34_c	0.415 ± 0.03
Sorafenib	0.588 ± 0.04

[a] All experiments were repeated three times. The results were expressed as the mean ± stander deviation (mean ± SD) calculated from three independent experiments (n = 3). P value < 0.05 was considered significant. IC_{50} values are the mean ± S.D. of three separate experiments.

2.2.3. Structure-Activity Relationship (SAR)

Investigation of results of the different biological tests (*in vitro* anti-proliferative activity and *in vitro* VEGFR-2 enzyme assay inhibition) revealed a range of potent VEGFR-2 inhibition activity. Five series of new quinazolines differentiated by incorporating a diverse of donor/acceptor groups such as a hydrazone, sulfonamide, acetamidobenzamide, 2-hydroxybenzolhydrazine, and thiosemicarbazone moieties have been designed using structure-activity relationships.

Generally, our results showed that some derivatives have high activity on either cell lines or VEGFR-2 compared to the lead compound Sorafenib. Among these derivatives, it was noticed that introduction of a hydrazone group (**16_f**) led to an increase in VEGFR-2 enzymatic activity (IC_{50} = 0.290 µg/mL) and anti-proliferative effect (IC_{50} = 1.88, 1.68, and 3.91 µM against HepG-2, HCT-116 and MCF-7 cell lines, respectively) Also, replacement of the urea entity of sorafenib by acetamidobenzamide (**28_b**) presented a higher VEGFR-2 inhibitory effect and an increased anti-tumor activity (IC_{50} = 0.380 µg/mL against VEGFR-2 and 4.12, 3.67, and 5.99 µM against HepG-2, HCT-116 and MCF-7 cell lines, respectively). Moreover, and according to our investigations, the

insertion of sulfonamide (**34$_a$** and **34$_c$**) instead of urea moiety increased enzymatic activity and appeared to be a new opportunity to develop VEGFR-2 inhibitors. On the other hand, when the sorafenib urea was replaced by thiosemicarbazone motif (**18**) it afforded a compound with almost equal activity compared to sorafenib (IC_{50} = 0.517 µg/mL against VEGFR-2 and 8.38, 8.32, and 9.89 µM against HepG-2, HCT-116 and MCF-7 cell lines, respectively). Unfortunately, neither the enzymatic inhibition nor the anti-tumor activities of the newly synthesized compound with hydroxybenzoyl hydrazine moiety (**31**) were enhanced (IC_{50} = 0.619 µg/mL against VEGFR-2 and 11.69, 10.76, and 14.38 µM against HepG-2, HCT-116 and MCF-7 cell lines, respectively).

Regarding hydrazone containing compounds, the most active inhibitor was **16$_f$** bearing a 2-chloro-5-nitrophenyl group as a hydrophobic tail (IC_{50} = 0.290 µg/mL against VEGFR-2 and 1.88, 1.68, and 3.91 µM against HepG-2, HCT-116 and MCF-7 cell lines, respectively). However, insertion of 2-hydroxyphenyl moiety as a hydrophobic tail produced compound **16$_e$** showed a decreased anti-proliferative effect (IC_{50} = 11.92, 12.37, and 15.44 µM against HepG-2, HCT-116 and MCF-7 cell lines, respectively). These results indicate that grafting a large electron withdrawing substituents at the terminal hydrophobic tail is beneficial for the activity.

Comparing the anticancer activities of acetamido benzamide derivatives of 2-mercapto-3-(4-methylphenyl)quinazolin-4(3*H*)-one showed that the activity of 4-chloro **28$_b$** (IC_{50} = 0.380 µg/mL against VEGFR-2 and 4.12, 3.67, and 5.99 µM against HepG-2, HCT-116 and MCF-7 cell lines, respectively) is superior than that expressed by sorafenib and better than 4-methyl **28$_c$** (IC_{50} = 19.02, 17.43, and 28.35 µM against HepG-2, HCT-116 and MCF-7 cell lines, respectively), and ester **28$_d$** (IC_{50} = 21.51, 17.02, and 23.74 µM against HepG-2, HCT-116 and MCF-7 cell lines, respectively), indicating that grafting electron withdrawing substituents at positions **4** is beneficial for activity.

For *N*-substituted benzene sulfonamide derivatives, it was found that compound incorporating *N*-acetyl derivative **34$_a$** (IC_{50} = 0.377 µg/mL against VEGFR-2 and 4.19, 6.14, and 6.79 µM against HepG-2, HCT-116 and MCF-7 cell lines, respectively) was more preferred biologically than that those having aromatic heterocyclic rings (**34$_b$** and **34$_c$**).

2.3. Molecular docking

The target compounds were docked into the active site of VEGFR-2 (PDB ID: 2OH4) to understand their binding mode. The reason we chose 2OH4 as receptor is that 2OH4 complex contains a urea containing ligand. Molecular insights based on molecular docking indicated favorable binding interactions of the newly synthesized compounds with the active site of VEGFR-2. Sorafenib was used as a reference compound. The distinctive binding pattern of sorafenib to VEGFR-2 kinase active site has been discussed and compared to the tested compounds.

^{1}N–H of the urea unit of sorafenib formed a hydrogen bond with Glu883 with distance of 1.68 Å. ^{3}N–H could also bind to the side chain carboxylate of Glu883 with distance of 1.59 Å. Moreover, carbonyl group was identified to be involved in a hydrogen bond interaction with the backbone NH of Asp1044 with distance of 1.74 Å. Besides, the phenyl group (spacer) between urea and oxygen acts as a hydrophobic moiety and interacts with the hydrophobic site (Lys866) in the hinge region. These results were the same as the reported data [74] **Fig. 5**.

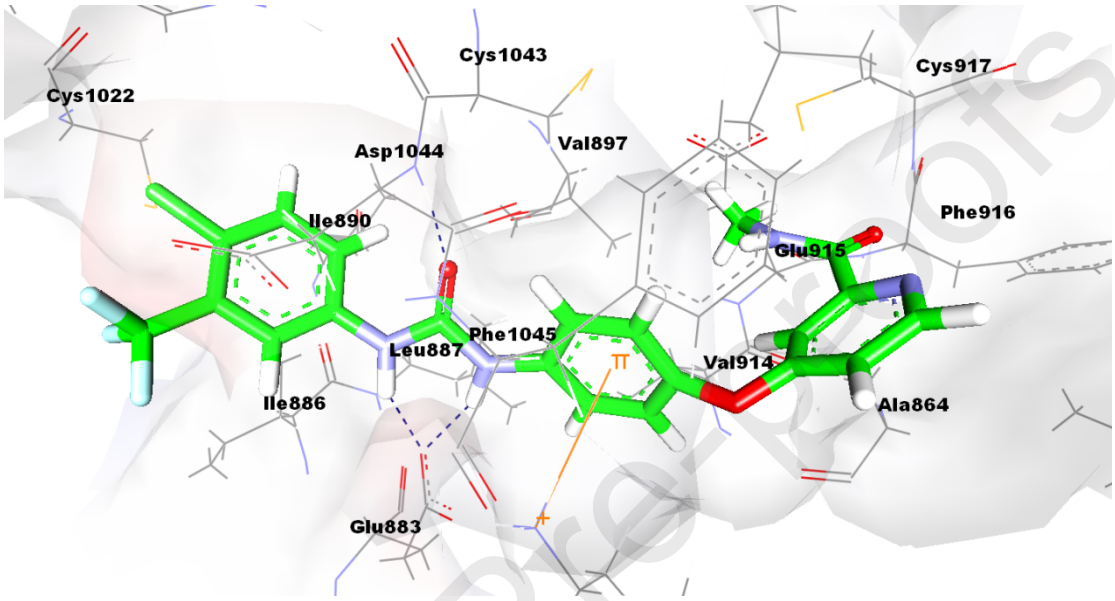

Fig. 5. The Predicted binding mode for sorafenib with the active site of VEGFR-2

Results of the docking study indicated that most of the target compounds showed a similar position and orientation inside the putative binding sites of VEGFR-2. The calculated ΔG (binding free energies) of the synthesized compounds and the reference drug against VEGFR-2 were summarized in **Table 3**.

The binding mode of compound **16$_f$** (affinity value of -58.02 kcal/mol), revealed that the N-H group of the hydrazono moiety formed hydrogen bond with Glu883 in the active site (2.45Å) while oxygen atom of the carbonyl group formed one hydrogen bond with Asp1044 with a distance of 2.52 Å. Additionally, the oxygen atom of carbonyl group of the quinazoline nucleus formed hydrogen bond with Asn921 (2.10 Å). Additionally, this compound formed three arene-arene interactions, one of which occurred between the central phenyl moiety (spacer) and Lys866, the other two cationic pi bonds were formed between quinazoline moiety and Arg1049 **Fig. 6 (A).** In order to compare their spatial orientations, superimposition of Sorafenib and 16f was performed and illustrated in **Fig. 6 (B).**

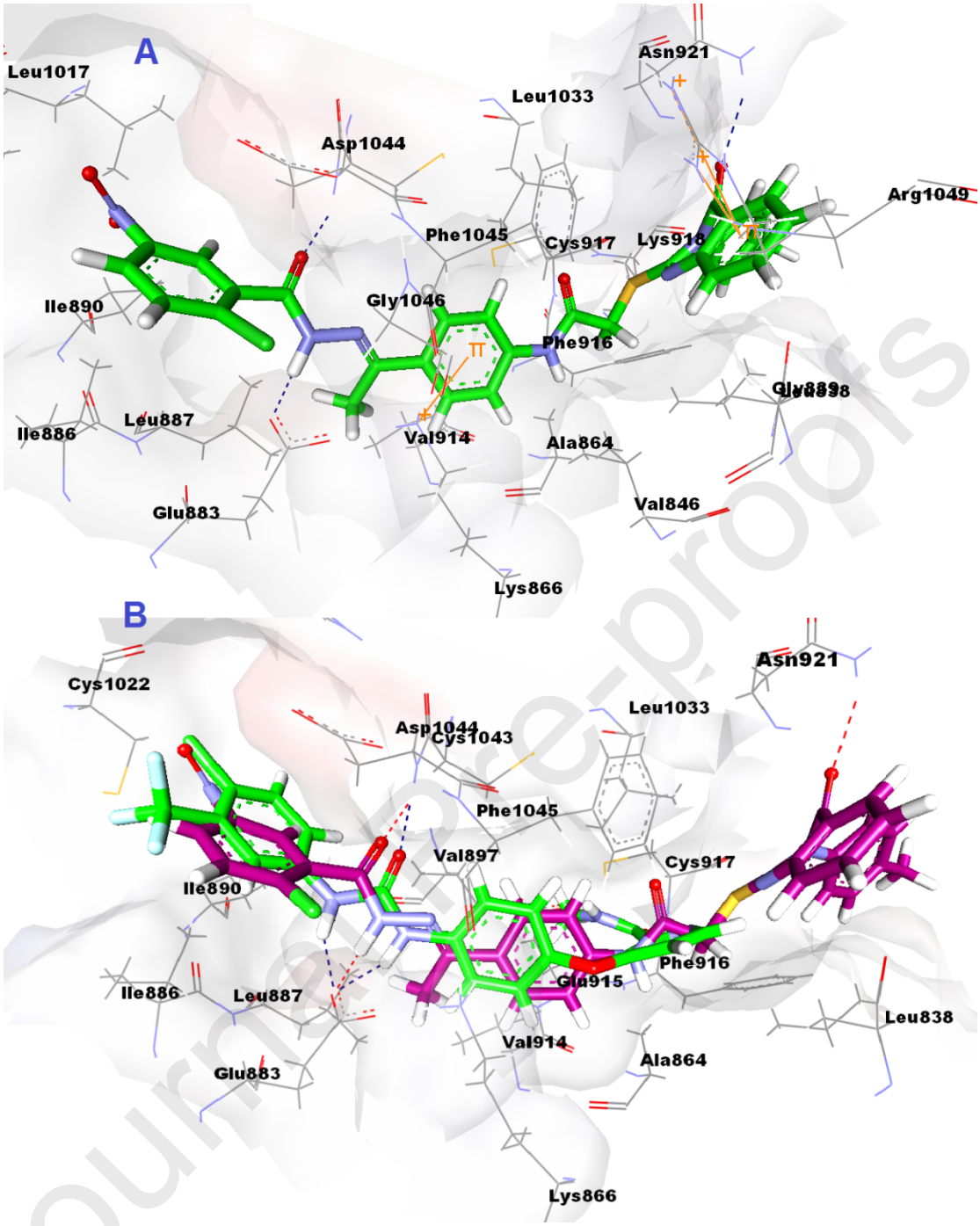

Fig. 6. (A). Predicted binding mode of compound **16$_f$** with the active site of VEGFR-2. **(B)**. Superimposing Sorafenib and 16f (Sorafenib in green color, **16$_f$** in maroon color).

Investigation of the top docking poses of compound **28$_b$** (affinity value of -51.47 kcal/mol), showed three hydrogen bond interactions in the active site of VEGFR-2. The oxygen atom of carbonyl group of the spacer formed hydrogen bond with Asp1044(1.97Å), while the N-H of the amide (spacer) formed two hydrogen bonds of 2.18, 2.47 Å with Glu883. This compound formed

tow arene-arene interaction, one of them is a cationic pi interaction with Phe916 and the other one formed between the phenyl of spacer and (Lys866) **Fig. 7**.

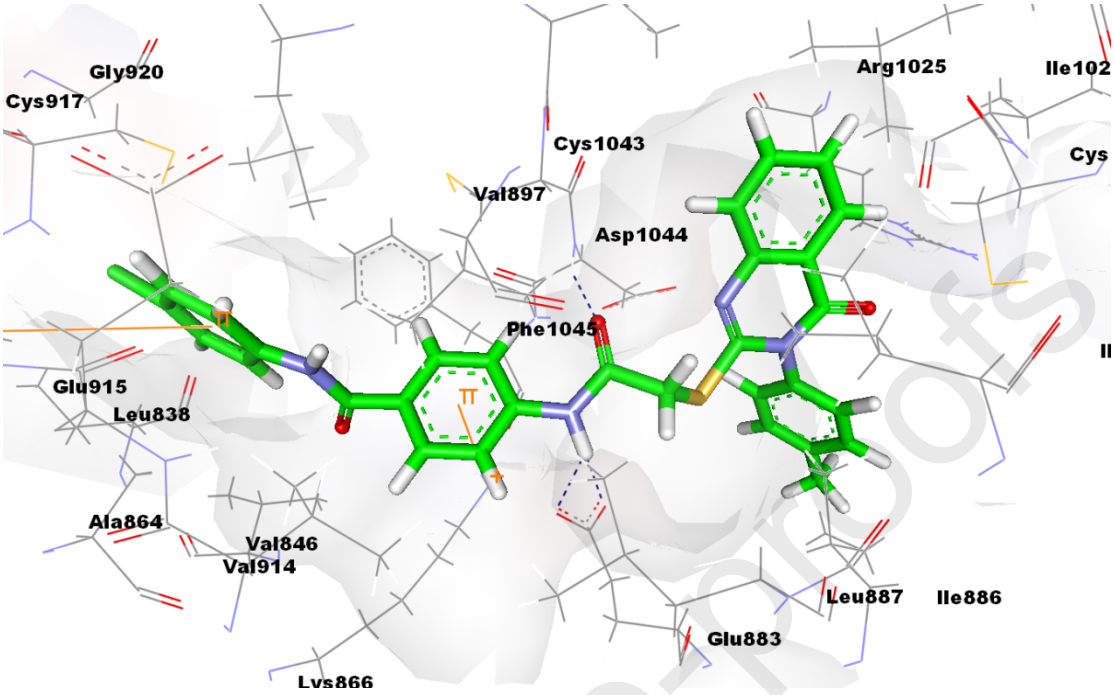

Fig. 7. Predicted binding mode of compound **28$_b$** with the active site of VEGFR-2.

The binding mode of compound **34$_a$** (affinity value of -51.79 kcal/mol), revealed that the N-H groups of the spacer moiety formed two hydrogen bonds with Glu883 in the active site (2.16 Å, 2.27 Å) while oxygen atom of the carbonyl group formed one hydrogen bond with Asp1044 with a distance of 2.31 Å. This compound formed one cationic pi bond with (Lys866) **Fig. 8.**

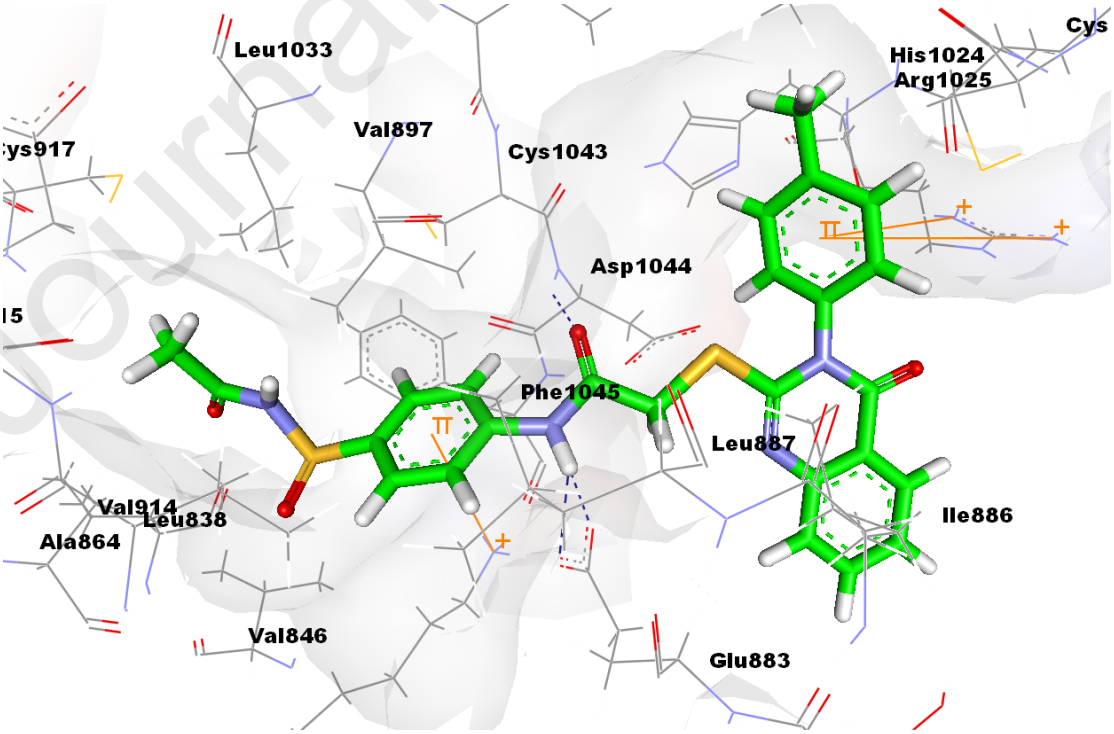

Fig. 8. Predicted binding mode of compound **34_a** with the active site of VEGFR-2.

Table 3: The calculated ΔG (binding free energies) of the synthesized compounds and reference drug against VEGFR-2 (ΔG in Kcal/mol)**.**

Comp.	ΔG [Kcal/mol]	Comp.	ΔG [Kcal/mol]
12	- 36.81	**28_a**	-34.42
16_a	- 39.00	**28_b**	- 51.47
16_b	- 35.26	**28_c**	-39.00
16_c	- 36.09	**28_d**	-42.18
16_d	- 36.35	**29**	- 28.81
16_e	-43.28	**31**	-26.27
16_f	-58.02	**34_a**	-51.79
18	-47.72	**34_b**	-32.48
26	-36.51	**34_c**	-51.13
27	-40.42	**Sorafenib**	-52.20

3. Conclusion

In summary, we have designed and synthesized nineteen final novel quinazoline-based derivatives incorporating, sulfonamide, hydrazono, acetamidobenzamide, 2-hydroxybenzoyl hydrazine and thiosemicarbazone moieties. The newly synthesized compounds were evaluated for their anti-proliferative activities against panel of three human cancer cell lines namely; hepatocellular carcinoma (HepG2), breast cancer (MCF-7) and colorectal carcinoma (HCT-116) using MTT assay. Compound **16_f** has emerged as the most active member with IC_{50} values of 1.88 ± 0.07, 1.68 ± 0.06, 3.91 ± 0.15 μM as it was 4.39, 5.73 and 1.96 times more active than doxorubicin (IC_{50} = 8.28 ± 0.33, 9.63 ± 0.38 and 7.67 ± 0.30 μM) and 3.88, 5.59 and 1.84 times more active than sorafenib (IC_{50} = 7.31 ± 0.29, 9.40 ± 0.37and 7.21 ± 0.28 μM) against HepG2, HCT-116 and MCF-7 cells, respectively. Also, compounds **18**, **28_b, 34_a** and **34_c** displayed excellent anti-proliferative activities against HepG2 and HCT-116 cell lines. In addition, the most potent compounds were examined for their VEGFR-2 inhibitory activities. Interestingly, the results of VEGFR-2 inhibition were consistent with that of the cytotoxicity data. Most of tested compounds

displayed superior to moderate inhibitory activity compared to the reference drug, sorafenib. Docking studies supported the previous results via prediction of the possible binding interactions of the designed compounds with VEGFR-2 active sites. The most active candidates may serve as useful lead compounds in the search for powerful and selective antineoplastic agents and deserve further investigations.

4. Experimental

4.1. Chemistry

Melting points were determined with a Gallen lamp melting point apparatus and are uncorrected. Silica gel Merck 60 F254 commercial plates were used for analytical TLC as well as UV light and/or with iodine to follow the course of the reaction. The structure of each compound was confirmed by IR (pye Unicam SP 1000 IR spectrophotometer), ^{1}H NMR (400 MHz, Bruker Biospin GmbH spectrophotometer) and ^{13}C NMR spectra (100 MHz, Bruker Biospin GmbH spectrophotometer). Chemicals shifts (δ) are reported in parts per million downfield from TMS, J values are in hertz, and the splitting patterns are abbreviated as follows: s, singlet; d, doublet; t, triplet; q, quartet; m, multiplet. The mass spectra were recorded on Varian MAT 311-A (70 e.v.).

Compounds 2-Mercapto-3-(4-methylphenyl)quinazolin-4(3H)-one **8** [75, 76], *N*-(4-Acetylphenyl)-2-chloroacetamide **11** [56], ethyl (un)substitutedbenzoate **14$_{a-f}$** [58], (un)substituted-benzoic acid hydrazides **15$_{a-f}$** [59, 60], 4-(2-chloroacetamido)benzoic acid **20** [62], 4-(2-chloroacetamido)-*N*-(substituted)benzamide **22-25** [63, 64, 77], *N*-(4-(2-Benzoylhydrazine-1-carbonyl)phenyl)-2-chloroacetamide **30** [63] and 2-chloro-*N*-(4-(*N*-(substituted) sulfamoyl) phenyl)acetamide **33$_{a-c}$** [66, 67] were obtained according to the reported procedures.

4.1.1. Potassium salts of 2-mercapto-3-(4methylphenyl) quinazolin-4(3H)-one (9)

To a mixture of 2-mercapto-3-(4-methylphenyl) quinazolin-4(3*H*)-one **8** (0.05 mol) potassium hydroxide (2.8 g, 0.05 mol) was added. The mixture was refluxed in absolute ethanol (50 ml) for 1.5 h. Upon cooling to room temperature, precipitated product was obtained, collected washed with diethyl ether (30 mL) and dried. Yield 92%; mp > 350 C.

4.1.2. N-(4-acetylphenyl)-2-((4-oxo-3-(4-methylphenyl)-3,4-dihydroquinazolin-2-yl)thio)acetamide (12)

A solution of the potassium salt **9** (0.01 mol) and *N*-(4-acetylphenyl)-2-chloroacetamide **11** (2.15 g, 0.01 mol) in DMF (50 ml) was heated on a water bath for 8 h. After cooling to room temperature, the reaction mixture was poured on crushed ice. The precipitate was collected by filtration, dried and crystalized from ethanol to give the corresponding target compound **12**.

Buff crystals (yield 85 %); m.p.: 168-170 ^{o}C; IR (KBr, ν cm^{-1}): 3234 (NH), 1670, 1685 (3C=O).; ^{1}H NMR (400 MHz, DMSO-*d6*) δ ppm; 2.42 (s, 3H, C**H$_3$**-C$_6$H$_5$), 2.55 (s, 3H, COCH$_3$), 4.11 (s, 2H, S-CH$_2$), 7.37-7.42 (m, 4H, Ar-H), 7.44 (t, 1H, Ar-H), 7.50 (d, 1H, *J* = 8.8 Hz, Ar-H), 7.74 (d, 2H, *J* = 7.6 Ar-H), 7.80 (t, 1H, Ar-H), 7.92 (d, 2H, *J* = 7.6 Hz, Ar-H), 8.06 (d, 1H, *J* = 8.8 Hz, Ar-H), 10.74 (s, 1H, NH, D$_2$O exchangeable).; MS (*m/z*): 443.17 (M$^+$, 17.95 %), 309.14 (100 %),; Anal. Calcd. For $C_{25}H_{21}N_3O_3S$ (443.13): C, 67.70; H, 4.77; N, 9.47; Found: C, 67.98; H, 4.83; N, 9.68%.

4.1.3. General procedure for synthesis of compounds (16$_{a-f}$)

A solution of *N*-(4-acetylphenyl)-2-((4-oxo-3-(4-methylphenyl)-3,4-dihydroquinazolin-2-yl)thio)acetamide **12** (0.001 mol) was treated with the appropriate prepared benzohydrazide derivatives namely, benzohydrazide, 2-chlorobenzohydrazide, 3-chlorobenzohydrazide, 4-chlorobenzohydrazide, 2-hydroxybenzohydrazide and 2-chloro-5-nitrobenzohydrazide **15$_{a-f}$** (0.001 mol) in ethanol (50 ml) in the presence of catalytic amount of glacial acetic acid and refluxed for 8 h. The resulting solids were filtered, washed with water (15 mL), dried and recrystallized from ethanol to afford the corresponding target compounds **16$_{a-f}$** respectively.

4.1.3.1. N-(4-(1-(2-Benzoylhydrazono)ethyl)phenyl)-2-((4-oxo-3-(4-methylphenyl)-3,4-dihydroquinazolin-2-yl)thio)acetamide 16$_a$

Pale yellow crystals (yield 83 %); m.p.: 188-190 ^{o}C; IR (KBr) cm^{-1}: 3421, 3310 (2NH), 1716, 1658 (3C=O).; ^{1}H NMR (DMSO.d_6, δ ppm): 2.34 (s, 3H, C**H$_3$**–C$_6$H$_5$), 2.42 (s, 3H, CH$_3$-C=N), 4.10 (s, 2H, -SCH$_2$), 7.35 (d, 2H, *J* = 6.4 Hz, Ar-H), 7.39 (d, 2H, *J* = 6.4 Hz, Ar-H), 7.47 (t, 1H, *J* = 6.0 Hz, Ar-H), 7.49-7.58 (m, 4H, Ar-H), 7.68 (d, 2H, *J* = 6.8 Ar-H), 7.80 -7.85 (m, 3H, Ar-H), 7.89 (d, 2H, *J* = 6.8 Hz, Ar-H), 8.07 (d, 1H, *J* = 6.4 Hz, Ar-H), 10.55 (s, 1H, CONH; D$_2$O exchangeable), 10.74 (s, 1H, NHCO; D$_2$O exchangeable); ^{13}C NMR: 19.03, 21.35, 37.83, 56.51, 119.07 (2C), 119.15, 120 (2C), 126.35, 126.46, 127.08, 127.40, 127.63, 128.30, 128.79, 129.59 (2C), 130.52 (2C), 131.90, 133.41, 134.58, 135.38 (2C), 140.19, 140.62, 147.59, 155.75, 157.69, 161.13, 166.47; DEPT135 NMR: 19.03 (2CH3), 21.35 (2CH3), 37.83 (2CH2), 119.07 (2CH), 119.15, 126.35, 126.46, 127.09, 127.39, 127.63, 128.29, 128.79, 129.59 (2CH), 130.52 (2CH), 131.92, 135.38 (2CH); Anal. Calcd. for $C_{32}H_{27}N_5O_3S$ (561.66): C, 68.43; H, 4.85; N, 12.47, Found: C, 68.61; H, 4.97; N,12.73 %.

4.1.3.2. N-(4-(1-(2-(2-Chlorobenzoyl)hydrazono)ethyl)phenyl)-2-((4-oxo-3-(4-methylphenyl)-3,4-dihydroquinazolin-2-yl)thio)acetamide 16$_b$

White crystals (yield 65 %); m.p.: 217-220 ^{o}C; IR (KBr) cm^{-1}: 3308, 3259 (2NH), 1712, 1701, 1656 (3C=O); ^{1}H NMR (DMSO.d_6, δ ppm): 2.26, 2.29 (2s, 3H, C**H$_3$** –C$_6$H$_5$), 2.41, 2.42 (2s, 3H,

CH_3-C=N) 4.07, 4.12 (2s, 2H, S-CH_2), 7.35-7.48 (m, 6H, Ar-H), 7.50-7.53 (m, 4H, Ar-H), 7.54 (dd, 1H, *J* = 6 Hz, Ar-H), 7.69 (d, 1H, *J* = 8.8 Hz, Ar-H), 7.77 (s, 1H, Ar-H), 7.85 (dd, 2H, *J* = 8.8, 8.0 Hz, Ar-H), 8.06 (dt, 1H, *J* = 6.4 Hz, Ar-H), 10.44, 10.56 (2s, 1H, CONH; D_2O exchangeable), 10.96, 11.20 (2s, 1H, NHCO, D_2O exchangeable).; ^{13}C NMR: 14.88, 19.04, 21.34, 37.83, 56.53, 119.01 (2C), 120.01, 126.35, 126.46, 127.08, 127.73 (2C), 129.59 (2C), 130.53 (2C), 132.99, 133.63, 135.37, 140.19 (2C), 140.39, 147.57, 147.60, 157.65, 157.69, 161.13, 161.15, 166.38, 166.50, 179.99; DEPT135 NMR: 14.01 ($1CH_3$), 14.889 ($1CH_3$), 19.04 ($1CH_3$), 21.35 ($1CH_3$), 37.82 ($1CH_2$), 56.53 ($1CH_2$), 118.99, 119.08 (2CH), 126.34, 126.46, 126.93, 127.08, 127.25, 127.56, 127.67 (2CH), 129.01, 129.26, 129.58 (2CH), 130.02, 130.52 (2CH), 130.70, 131.53, 135.37; Anal. Calcd. for $C_{32}H_{26}ClN_5O_3S$ (596.10): C, 64.48; H, 4.40; N, 11.75 Found: C, 64.60; H, 4.37; N, 12.01%.

***4.1.3.3. N-(4-(1-(2-(3-Chlorobenzoyl)hydrazono)ethyl)phenyl)-2-((4-oxo-3-(4-methylphenyl)-3,4-dihydroquinazolin-2-yl)thio)acetamide* 16$_c$**

Beige crystals (yield 58 %); m.p.: 221-223 ^oC; IR (KBr) cm^{-1} :3337, 3266 (2 NH), 1718, 1685 (3C═O).; ^1H NMR (DMSO.d_6, δ ppm): 2.34 (s, 3H, C**H$_3$**-C_6H_5), 2.43 (s, 3H, CH_3-C=N) 4.10 (s, 2H, S-CH_2), 7.34 (d, 2H, *J* = 8.4, 8.0 Hz, Ar-H), 7.39 (d, 2H, *J* = 8.4 Hz, Ar-H), 7.44 (t, 1H, *J* = 8.0, 8.4 Hz, Ar-H), 7.53 (d, 2H, *J* = 8.4 Hz, Ar-H), 7.64 (d, 2H, *J* = 9.2 Hz, Ar-H), 7.68 (d, 1H, Ar-H), 7.79-7.84 (m, 4H, Ar-H), 7.92 (s, 1H, Ar-H), 8.08 (d, 1H, *J* = 9.2 Hz, Ar-H), 10.53 (s, 1H, CONH; D_2O exchangeable), 10.83 (s, 1H, NHCO, D_2O exchangeable).; ^{13}C NMR; 21.34, 37.80, 119.1 (4C), 120.00, 126.34, 126.47 (2C), 127.09 (2C), 127.71, 129.59 (4C), 130.51 (4C), 130.79, 133.29, 133.62 (2C), 135.38, 140.18 (2C), 147.59, 157.68, 161.13, 166.46; DEPT135 NMR; 14.99, 21.34, 37.80, 119.09 (2CH), 126.34, 126.47, 127.08 (2CH), 127.69, 129.58 (2CH), 130.51 (2CH), 135.38 Anal. Calcd. for $C_{32}H_{26}ClN_5O_3S$ (596.10): C, 64.48; H, 4.40; N, 11.75; Found: C, 64.67; H, 4.53; N, 11.88 %.

4.1.3.4. N-(4-(1-(2-(4-Chlorobenzoyl)hydrazono)ethyl)phenyl)-2-((4-oxo-3-(4-methylphenyl)-3,4-dihydroquinazolin-2-yl)thio)acetamide 16$_d$

White crystals (yield 79 %); m.p.: 247 ^oC; IR (KBr) cm^{-1}: 3336, 3256 (2 NH), 1751, 1715, 1651 (3C=O).; ^1H NMR (DMSO.d_6, δ ppm): 2.33 (s, 3H, C**H$_3$**-C_6H_5), 2.43 (s, 3H, CH_3-C=N) 4.11 (s, 2H, S-CH_2), 7.35 (dd, 2H, *J* = 8.4, 8.0 Hz, Ar-H), 7.39 (dd, 2H, *J* = 8.4, 8.0 Hz, Ar-H), 7.44 (t, 1H, *J* = 7.6 Hz, Ar-H), 7.54 (d, 2H, *J* = 8.0 Hz, Ar-H), 7.59 (d, 2H, *J* = 8.0 Hz, Ar-H), 7.67 (d, 1H, *J* = 8.4 Hz, Ar-H), 7.79 (t, 3H, *J* = 8.0 Hz, Ar-H), 7.92-7.95 (m, 2H, Ar-H), 8.06 (d, 1H, *J* = 8.0 Hz, Ar-H), 10.56 (s, 1H, CONH; D_2O exchangeable), 10.81 (s, 1H, NHCO; D_2O exchangeable).;^{13}C NMR; 21.34, 37.84, 119.12 (2C), 120.01 (2C), 126.35, 126.45 (2C), 127.08 (2C), 127.64, 128.81

(2C), 129.59 (2C), 130.25, 130.51 (2C), 133.34 (2C), 133.63 (2C), 135.36 (2C), 140.18 (2C), 147.60, 157.69, 161.13, 166.45; DEPT135 NMR; 14.90 ($1CH_3$), 21.35 ($1CH_3$), 37.84 ($1CH_2$), 119.11 (2CH), 126.35, 126.46 (2CH), 127.09 (2CH), 127.64, 128.81, 129.59 (2CH), 130.25, 130.51 (2CH), 135.37 (2CH). Anal. Calcd. For: $C_{32}H_{26}ClN_5O_3S$ (596.10): C, 64.48; H, 4.40; N, 11.75; Found: C, 64.65; H, 4.51; N, 11.92 %.

4.1.3.5. N-(4-(1-(2-(2-Hydroxybenzoyl)hydrazono)ethyl)phenyl)-2-((4-oxo-3-(4-methylphenyl)-3,4-dihydroquinazolin-2-yl)thio)acetamide 16_e

Pale yellow crystals (yield 75 %); m.p.: 203-206 ^oC; IR (KBr) cm^{-1}: 3628 (OH), 3447, 3276 (2NH), 1716, 1686, (3C=O).; ^1H NMR (DMSO.d_6, δ ppm): 2.31 (s, 3H, C**H**$_3$ –C_6H_5), 2.42 (s, 3H, CH_3-C=N), 4.11 (s, 2H, S-CH_2), 7.37 (d, 2H, *J* = 8.4 Hz, Ar-H), 7.39 (d, 2H, *J* = 8.4 Hz, Ar-H), 7.46 (t, 1H, *J* = 7.6 Hz, Ar-H), 7.54 (d, 1H, *J* = 8.0 Hz, Ar-H), 7.59 (d, 2H, *J* = 8.4 Hz, Ar-H), 7.67 (d, 2H, *J* = 8.4 Hz, Ar-H), 7.79 (d, 2H, *J* = 8.4 Hz, Ar-H), 7.84 (t, 1H, Ar-H), 7.92 (d, 2H, *J* = 8.4 Hz, Ar-H), 8.06 (dd, 1H, *J* = 8.0 Hz, Ar-H), 10.54 (s, 1H, CONH; D_2O exchangeable), 11.33 (s,1H, NHCO; D_2O exchangeable), 11.84 (s, 1H, OH; D_2O exchangeable); ^{13}C NMR; 14.14, 21.34, 37.85, 117.37, 118.34, 119.15 (2C), 120.01(2C), 126.35, 126.44, 127.08, 127.60 (2C), 129.59 (2C), 130.51(2C), 130.96, 133.26, 133.63, 133.76, 135.35, 140.18, 140.55, 147.60, 152.55, 157.14, 157.68, 161.13, 162.56, 166.46; DEPT135 NMR: 14.14 ($1CH_3$), 21.34 ($1CH_3$), 37.85, 117.37, 119.14 (2CH), 120.05, 126.35, 126.44, 127.08, 127.60 (2CH), 129.59 (2CH), 130.51 (2CH), 130.96, 133.75, 135.35; Mass (*m/z*): 577.53 (M^+, 11.01 %), 526.21 (100 %).; Anal. Calcd. for $C_{32}H_{27}N_5O_4S$ (577.66): C, 66.54; H, 4.71; N, 12.12; Found: C, 66.41; H, 4.89; N, 12.34%.

4.1.3.6. N-(4-(1-(2-(2-Chloro-5-nitrobenzoyl)hydrazono)ethyl)phenyl)-2-((4-oxo-3-(4-methylphenyl)-3,4-dihydroquinazolin-2-yl)thio)acetamide 16_f

Orange crystals (yield 87 %); m.p.: 185-187 ^oC; IR (KBr) cm^{-1}: 3481 (NH), 1725, 1672 (3C═O).; ^1H NMR (DMSO.d_6, δ ppm): 2.31 (s, 3H, C**H**$_3$ –C_6H_5), 2.43 (s, 3H, CH_3–C=N), 4.10 (s, 2H, S-CH_2), 7.34 (d, 2H, *J* = 8.0 Hz, Ar-H), 7.39 (d, 2H, *J* = 8.0 Hz, Ar-H), 7.44 (t, 1H, *J* = 6.8, 8.0 Hz, Ar-H), 7.53 (d, 1H, *J* = 8.8 Hz, Ar-H), 7.66 (d, 2H, *J* = 8.0 Hz, Ar-H), 7.81 (t, 1H, *J* = 7.6, 8.8 Hz, Ar-H), 7.89 (d, 2H, *J* = 8.4 Hz, Ar-H), 8.03 (d, 1H, *J* = 8.0 Hz, Ar-H), 8.05 (d, 1H, *J* = 8.0 Hz, Ar-H), 8.28 (s, 1H, OH; D_2O exchangeable), 10.56 (s, 1H, CONH; D_2O exchangeable), 10.83 (s, 1H, NHCO, D_2O exchangeable).; Mass (*m/z*) : 641.12 (M^+, 35.65 %), 367.70 (100 %).; Anal. Calcd. for $C_{32}H_{25}CLN_6O_5S$ (641.10): C, 59.95; H, 3.93; N, 13.11; Found: C, 60.13; H, 4.07; N, 13.37 %.

4.1.4. N-(4-(1-(2-Carbamothioylhydrazono)ethyl)phenyl)-2-((4-oxo-3-(4-methylphenyl)-3,4-dihydroquinazolin-2-yl)thio)acetamide 18

A solution of *N*-(4-acetylphenyl)-2-((4-oxo-3-(4-methylphenyl)-3,4-dihydroquinazolin-2-yl)thio)acetamide **12** (0.001 mol) in ethanol (50 mL) was treated with thiosemicarbazide (0.001 mol) in the presence of catalytic amount of glacial acetic acid. The solution was refluxed for 8 h. Resulting solid was filtered, washed with water (15 mL), dried and crystallized from ethanol.

Pale green solid (yield 71 %); m.p.: 221-223^{o}C; IR (KBr) cm^{-1}: 3421 (NH_2), 3340, 3295 (2 NH), 1734, 1675 (2C=O).; ^{1}H NMR (DMSO.d_6, δ ppm): 2.26 (s, 3H, C**H**$_3$ –C_6H_5), 2.43 (s, 3H, CH_3-C=N), 4.09 (s, 2H, S-CH_2), 7.34 (d, 2H, *J* = 8.0, Ar-H), 7.39 (d, 2H, *J* = 8.4 Hz, Ar-H), 7.46 (t, 1H, *J* = 8.0 Hz, Ar-H), 7.53 (d, 1H, *J* = 8.8 Hz, Ar-H), 7.63 (d, 2H, *J* = 8.0 Hz, Ar-H), 7.81 (t, 1H, *J* = 8.8 Hz, Ar-H), 7.89 (d, 1H, *J* = 8.8 Hz, Ar-H), 7.91 (s, 2H, NHCSN**H**$_2$, D_2O exchangeable), 8.06 (d, 1H, *J* = 8.0 Hz, Ar-H), 8.25 (d, 1H, J = 8.0 Hz.Ar-H), 10.14 (s, 1H, CON**H**, D_2O exchangeable), 10.56 (s, 1H, N**H**$CSNH_2$, D_2O exchangeable); ^{13}C NMR; 19.03, 21.34, 37.88, 119.04 (2C), 119.99, 126.31, 126.44, 127.08, 127.72 (2C), 129.57 (2C), 130.51 (2C), 132.98, 133.60, 135.33, 140.18, 140.38, 147.58, 147.91, 157.67, 161.13, 166.41, 179.22; DEPT135 NMR; 19.03 ($1CH_3$), 21.34 ($1CH_3$), 37.88 (CH_2), 119.01 (2CH), 126.32, 126.44, 127.08, 127.72(2CH), 129.57 (2CH), 130.52 (2CH), 135.33; Mass (*m/z*): 516.86 (M^+, 36.41 %), 266.96 (100 %).; Anal. Calcd. for $C_{26}H_{24}N_6O_2S_2$ (516.64); C, 60.45; H, 4.68; N, 16.27; Found: C, 60.71; H, 4.86; N, 16.49 %.

4.1.5. General procedure for preparation of target compounds 26-29

A mixture of the potassium salt of 2-mercapto-3-(4-methylphenyl)quinazolin-4(3*H*)-one **9** (0.01mol) and the appropriate 4-(2-chloroacetamido)-*N*-(substituted)benzamide derivatives **22, 23, 24$_{a-d}$** or **25** (0.01 mol) in DMF (50 ml) was heated on a water bath for 8 h. After cooling to room temperature, the reaction mixture was poured onto crushed ice. The precipitate was collected by filtration, dried and crystalized from ethanol to give the corresponding target compound **26, 27, 28$_{a-d}$** and **29** respectively.

4.1.5.1. N-Cyclohexyl-4-(2-((4-oxo-3-(4-methylphenyl)-3,4-dihydroquinazolin-2-yl)thio) acetamido)benzamide 26

White crystals (yield 63 %); m.p.: 215-217 ^{o}C; IR (KBr) cm^{-1}: 3321, 3179 (2NH), 1681 (C=O).; ^{1}H NMR (DMSO.d_6, δ ppm): 1.10 (m, 2H, CH_2 of cyclohexyl), 1.27 (m, 2H, CH_2 of cyclohexyl), 1.58 (m, 2H, CH_2 of cyclohexyl), 1.72 (m, 2H, CH_2 of cyclohexyl), 1.79 (m, 2H, CH_2 of cyclohexyl), 2.48 (s, 3H, C**H**$_3$ –C_6H_5), 3.73 (m, 1H, C**H**- cyclohexyl), 4.09 (s, 2H, S-CH_2), 7.36-7.52 (m, 6H, Ar-H), 7.66 (d, 2H, Ar-H), 7.67 (d, 1H, *J* = 8.4 Hz, Ar-H), 7.79 (d, 2H, Ar-H), 7.74 (s, 1H, S-CH_2CON**H**cyclohexyl; D_2O exchangeable), 8.07 (d, 1H, *J* = 8.0 Hz ,Ar-H), 10.57 (s, 1H,

CONH; D_2O exchangeable).; Anal. Calcd. for $C_{30}H_{30}N_4O_3S$ (526.66): C, 68.42; H, 5.74; N, 10.64 Found: C, 68.58; H, 5.81; N, 10.43 %.

4.1.5.2. N-Benzyl-4-(2-((4-oxo-3-(4-methylphenyl)-3,4-dihydroquinazolin-2-yl)thio)acetamido) benzamide 27

Beige crystals (yield 63 %); m.p.: 215 ^oC; IR (KBr) cm^{-1}: 3308 (2 NH), 1701, 1658 (3C=O).; ^1H NMR (DMSO.d_6, δ ppm): 2.52 (s, 3H, C**H**$_3$ –C_6H_5), 4.12 (s, 2H, S-CH_2), 4.49 (s, 2H, C**H**$_2$ - C_6H_5), 7.22–7.39 (m, 10H, Ar-H), 7.67 (s, 3H, Ar-H), 7.84 (s, 3H, Ar-H), 8.07 (d, 1H, *J* = 8.0 Hz, Ar-H), 8.96 (s, 1H, N**H**CH_2 –C_6H_5), 10.42 (s, 1H, S-CH_2CON**H**; D_2O exchangeable); Anal. Calcd. For $C_{31}H_{26}N_4O_3S$ (534.63): C, 69.64; H, 4.90; N, 10.48 Found: C, 69.91; H, 4.78; N, 10.63 %.

4.1.5.3. 4-(2-((4-Oxo-3-(4-methylphenyl)-3,4-dihydroquinazolin-2-yl)thio)acetamido)-N-phenyl benzamide 28$_a$

White crystals (yield 77 %); m.p.: 244-245 ^oC; IR (KBr) cm^{-1}: 3300, 3194 (2NH), 1697, 1672 (3C=O).; ^1H NMR (DMSO.d_6, δ ppm): 2.42 (s, 3H, C**H**$_3$ –C_6H_5), 4.14 (s, 2H, S-CH_2), 7.07 (t, 1H, *J* = 8.0 Hz, Ar-H), 7.32-7.46 (m, 7H, Ar-H), 7.54 (d, 1H, *J* = 8.0 Hz, Ar-H), 7.76-7.80 (m, 5H, Ar-H), 7.97 (d, 2H, *J* = 8.0 Hz, Ar-H), 8.07 (d, 1H, *J* = 8.0 Hz, Ar-H), 10.14 (s, 1H, S-CH_2CON**H**; D_2O exchangeable), 10.67 (s, 1H, NHCO; D_2O exchangeable); ^{13}C NMR; 21.34, 37.88, 118.81 (2C), 120.03, 120.82 (2C), 123.96, 126.34, 126.46, 127.11, 129.01 (2C), 129.17 (2C), 129.59 (2C), 129.95, 130.53 (2C), 133.63, 135.34, 139.74, 140.2, 142.36, 147.6, 157.67, 161.14, 165.32, 166.77 DEPT135 NMR; 21.35 (1CH_3), 37.88 (1CH_2), 118.8 (2CH), 120.82 (2CH), 123.96, 126.33, 126.46, 127.11, 129.02 (2CH), 129.18 (2CH), 129.59 (2CH), 130.52 (2CH), 135.34; Anal. Calcd. for $C_{30}H_{24}N_4O_3S$ (520.61): C, 69.21; H, 4.65; N, 10.76 Found: C, 69.40; H, 4.59; N, 10.94 %.

4.1.5.4. N-(4-Chlorophenyl)-4-(2-((4-oxo-3-(4-methylphenyl)-3,4-dihydro-quinazolin-2-yl)thio) acetamido)benzamide 28$_b$

Brown crystals (yield 56 %); m.p.: 239-241 ^oC; IR (KBr) cm^{-1}: 3313, 3255 (2NH), 1700, 1671 (C=O).; ^1H NMR (DMSO.d_6, δ ppm): 2.43 (s, 3H, C**H**$_3$ –C_6H_5), 4.12 (s, 2H, S-CH_2), 6.72 (t, 1H, *J* = 7.2 Hz, Ar-H), 6.78 (d, 2H, *J* = 7.6 Hz, Ar-H), 7.13 (dd, 2H, *J* = 7.2, 8.4 Hz, Ar-H), 7.35 (d, 2H, *J* = 6.4 Hz, Ar-H), 7.40 (d, 2H, *J* = 6.4 Hz, Ar-H), 7.46 (dd, 1H, *J* = 8.0, 7.2 Hz, Ar-H), 7.53 (d, 1H, *J* = 8.0 Hz, Ar-H), 7.71 (d, 2H, *J* = 8.8 Hz, Ar-H), 7.89 (d, 2H, J = 8.8 Hz, Ar-H), 8.07 (d, 1H, *J* = 8.0 Hz, Ar-H), 10.26 (s, 1H, S-CH_2CON**H**; D_2O exchangeable), 10.63 (d, 1H, N**H**-C_6H_5; D_2O exchangeable).; ^{13}C NMR; 21.34, 37.81, 112.8 (2C), 118.91 (2C), 119.07, 120, 126.33, 126.49, 127.09, 128.12, 128.75 (2C), 129.17 (2C), 129.58 (2C), 130.53 (2C), 133.6, 135.38, 140.21, 142.35, 147.58, 150.05, 157.65, 161.14, 166.27, 166.75, DEPT135 NMR; 21.34 (1CH_3), 37.82 (1CH_2), 112.8 (2CH), 118.91 (2CH), 119.07, 126.33, 126.49, 127.1, 128.76 (2CH), 129.17 (2CH), 129.58

(2CH), 130.53 (2CH), 135.38; Anal. Calcd. for $C_{30}H_{23}ClN_4O_3S$ (555.05): C, 64.92; H, 4.18; N, 10.09 Found: C, 65.13; H, 4.29; N, 10.24 %.

4.1.5.5. 4-(2-((4-Oxo-3-(4-methylphenyl)-3,4-dihydroquinazolin-2-yl)thio)acetamido)-N-(4-methylphenyl) benzamide 28$_c$

Grey crystals (yield 84 %); m.p.: 228-230 ^oC; IR (KBr) cm^{-1}: 3310 (NH), 1697, 1722 (3C═O).; ^1H NMR (DMSO.d_6, δ ppm): 2.27 (s, 3H, C**H$_3$** –C_6H_5), 2.43 (s, 3H, C**H$_3$**-C_6H_5-NH), 4.11 (s, 2H, S-CH_2), 7.13 (d, 2H, *J* = 7.6 Hz, Ar-H), 7.35 (d, 2H, *J* = 8.0 Hz, Ar-H), 7.39 (d, 2H, *J* = 8.0 Hz, Ar-H), 7.44 (t, 1H, *J* = 7.6 Hz, Ar-H), 7.53 (d, 1H, *J* = 8.0 Hz, Ar-H), 7.63 (d, 2H, *J* = 8.0 Hz, Ar-H), 7.73 (d, 2H, *J* = 8.4 Hz, Ar-H), 7.81 (t, 1H, *J* = 7.6 Hz, Ar-H), 7.93 (d, 2H, *J* = 8.4 Hz, Ar-H), 8.06 (d, 1H, *J* = 8.0 Hz, Ar-H), 10.05 (s, 1H, CONH; D_2O exchangeable), 10.65 (s, 1H, CH_2CON**H**; D_2Oexchangeable); ^{13}C NMR; 20.95, 21.34, 37.83, 118.74 (2C), 120, 120.81 (2C), 126.32, 126.48, 127.1, 129.09 (2C), 129.42 (2C), 129.58 (2C), 129.98, 130.52 (2C), 132.9, 133.6, 135.37, 137.16, 140.2, 142.25, 147.58, 157.67, 161.12, 165.09, 166.75; DEPT135 NMR; 20.95 ($1CH_3$), 21.34 ($1CH_3$), 37.83 ($1CH_2$), 118.73 (2CH), 120.81 (2CH), 126.31, 126.47, 127.09, 129.09 (2CH), 129.41 (2CH), 129.58 (2CH), 130.52 (2CH), 135.36 Anal. Calcd. for $C_{31}H_{26}N_4O_3S$ (534.63): C, 69.64; H, 4.90; N, 10.48; Found: C, 69.85; H, 4.78; N, 10.67 %.

4.1.5.6. Ethyl-4-(4-(2-((4-oxo-3-(4-methylphenyl)-3,4-dihydroquinazolin-2-yl)thio) acetamido) benzamido)benzoate 28$_d$

Beige crystals (yield 87 %); m.p.: 155-158 ^oC; IR (KBr) cm^{-1}: 3462, 3343 (2NH), 1672, 1657 (3C=O amide), 1709 (C=O ester).; ^1H NMR (DMSO.d_6, δ ppm): 1.30 (t, 3H, *J* = 6.4 Hz, CH_2C**H$_3$**), 2.43 (s, 3H, C**H$_3$** -C_6H_5), 4.12 (s, 2H, S-CH_2), 4.27 (q, 2H, *J* = 6.4 Hz, C**H$_2$**CH_3), 7.35 (d, 2H, *J* = 8.0 Hz, Ar-H), 7.40 (d, 2H, *J* = 8.0 Hz, Ar-H), 7.44 (t, 1H, *J* = 7.6 Hz, Ar-H), 7.52 (d, 1H *J* = 8.4 Hz, Ar-H), 7.75 (d, 2H, *J* = 8.8 Hz, Ar-H), 7.79 (t, 2H, *J* = 7.6 Hz, Ar-H), 7.95–7.98 (m, 5H, Ar-H), 8.06 (d, 1H, *J* = 8.0 Hz, Ar-H), 10.44 (s, 1H, S-CH_2CON**H**; D_2O exchangeable), 10.69 (s, 1H, CONH; D_2O exchangeable).; ^{13}C NMR; 14.69, 21.34, 37.83, 60.91, 118.7 (2C), 119.95 (2C), 120 (2C), 124.87, 126.31, 126.49 (2C), 127.11, 129.39 (2C), 129.59 (2C), 130.51 (4C), 133.61, 135.38, 140.21, 142.66, 144.19, 147.58, 161.12, 165.7, 165.84, 166.83; DEPT135 NMR; 14.69($1CH_3$), 21.34 ($1CH_3$), 37.83 ($1CH_2$), 60.91 ($1CH_2$), 118.77 (2CH), 119.95 (2CH), 126.31, 126.48 (2CH), 127.1, 129.38 (2CH), 129.59 (2CH), 130.51 (2CH), 132.04, 135.37; Anal. Calcd. For $C_{33}H_{28}N_4O_5S$ (592.67): C, 66.88; H, 4.76; N, 9.45 **Found**: C, 67.12; H, 4.83; N, 9.66 %.

4.1.5.7. 2-((4-Oxo-3-(4-methylphenyl)-3,4-dihydroquinazolin-2-yl)thio)-N-(4(2-phenyl hydrazine-1-carbonyl)phenyl)acetamide 29

Pale brown crystals (yield 55 %); m.p.: 225-227 ^{o}C; IR (KBr) cm^{-1}: 3303, 3179 (2NH), 1677, 1659 (3C=O).; ^{1}H NMR (DMSO.d_6, δ ppm): 2.41 (s, 3H, C**H**$_3$-C$_6$H$_5$), 4.15 (s, 2H, S-CH$_2$), 7.37-7.45 (m, 6H, Ar-H), 7.54 (d, 1H, J = 8.0 Hz, Ar-H), 7.77-7.81 (m, 3H, Ar-H), 7.8 (d, 3H, J = 8.8 Hz, Ar-H), 7.97 (d, 3H, J = 8.0 Hz, Ar-H), 8.07 (d, 1H, J = 8.8 Hz, Ar-H), 10.28 (s, 1H, NHN**H**-C$_6$H$_5$; D$_2$O exchangeable) 10.50 (s, 1H, S-CH$_2$CON**H**; D$_2$O exchangeable), 10.70 (s, 1H, CONHNH-C$_6$H$_5$; D$_2$O exchangeable); ^{13}C NMR; 21.34, 37.90, 118.81 (2C), 120.01, 122.26 (2C), 126.33, 127.11, 127.60, 128.92 (2C), 129.18, 129.24 (2C), 129.57 (2C), 130.52 (2C), 133.61, 135.31, 138.71, 140.2, 142.51, 147.59, 157.64, 161.15, 165.4, 166.82, 168.46; DEPT135 NMR; 21.34 (CH$_3$), 37.9 (CH$_2$), 118.81 (2C), 122.26 (2C), 126.33, 126.43, 127.11, 128.92 (2C), 129.18, 129.24 (2C), 129.57 (2C), 130.53 (2C), 135.32.; Mass (*m/z*): 535.46 (M$^+$, 5.82 %), 526.15 (100 %).; Anal. Calcd. for $C_{30}H_{25}N_5O_3S$ (535.62): C, 67.27; H, 4.70; N, 13.08 Found: C, 67.40; H, 4.87; N, 13.25 %.

4.1.6. N-(4-(2-(2-Hydroxybenzoyl)hydrazine-1-carbonyl)phenyl)-2-((4-oxo-3-(4-methylphenyl)-3,4-dihydro quinazolin-2-yl)thio)acetamide 31

A mixture of the potassium salt of 2-mercapto-3-(4-methylphenyl)quinazolin-4(3*H*)-one **9** (3.48 g, 0.01 mol) and *N*-(4-(2-benzoylhydrazine-1-carbonyl)phenyl)-2-chloroa-cetamide **30** (0.01 mol) in DMF (50 ml) was heated on a water bath for 8 h. After cooling to room temperature, reaction mixture was poured onto crushed ice. The formed precipitate was filtered, dried and crystalized from ethanol to give the corresponding target compound **31**.

Brown crystals (yield 61 %); m.p.: 260-263 ^{o}C; IR (KBr) cm^{-1}: 3262 (OH), 3184, 3112 (3NH), 1733, 1665 (3C=O).; ^{1}H NMR (DMSO.d_6, δ ppm): 2.42 (s, 3H, C**H**$_3$-C$_6$H$_5$), 4.12 (s, 2H, S-CH$_2$), 6.93–6.99 (m, 3H, Ar-H), 7.35–7.41 (m, 2H, Ar-H), 7.44 (t, 1H, J = 8.0 Hz, Ar-H), 7.52 (d, 1H, J = 8.4 Hz, Ar-H), 7.73 (d, 3H, J = 8.0 Hz, Ar-H), 7.79 (t, 1H, J = 7.6 Hz, Ar-H), 7.92 (d, 4H, J = 8.0 Hz, Ar-H), 8.07 (d, 1H, J = 8.0 Hz, Ar-H), 10.47 (s, 1H, CONH; D$_2$O exchangeable), 10.59 (s, 1H, OHC$_6$H$_5$; D$_2$O exchangeable), 10.68 (s, 2H, CONHNHCO; D$_2$O exchangeable); ^{13}C NMR; 21.34, 36.60, 115.09, 117.89 (2C), 118.90, 118.99 (2C), 119.44, 120, 126.48, 127.35, 128.76 (2C), 128.98 (2C), 129.58, 130.52, 133.61, 134.59, 135.39, 140.21, 142.66, 147.58, 157.65, 159.83, 161.14, 165.45, 166.84, 168.20, 168.45; DEPT135 NMR; 21.34 (CH$_3$), 36.60 (CH$_2$), 117.89 (2CH), 118.99 (2CH), 119.44, 126.33, 126.48, 127.09, 128.76 (2CH), 128.98 (2CH), 129.03, 129.58, 130.52 ,134.59, 135.39; Mass (*m/z*): 579.38 (M$^+$, 40.13 %), 250.42 (100 %).; Anal. Calcd. for $C_{31}H_{25}N_5O_5S$ (579.63): C, 64.24; H, 4.35; N, 12.08 Found: C, 64.48; H, 4.31; N, 12.39 %.

4.1.7. General procedure for preparation of target compounds 34$_{a-c}$

To a solution of the potassium salt of 2-mercapto-3-(4-methylphenyl)quinazolin-4(3*H*)-one **9** (3.5 g, 0.002mol) in DMF (50 mL) the appropriate 2-chloro-*N*-[4-(*N*-(substituted)sulfamoylphenyl] acetamides $\mathbf{33_{a-c}}$ (0.002 mol) was added. The mixture was heated on a water bath for 12 h. After cooling to room temperature, the reaction mixture was poured onto crushed ice. The precipitated solids were filtered, dried and crystalized from ethanol to give the target compounds $\mathbf{33_{a-c}}$.

4.1.7.1. N-(4-(N-Acetylsulfamoyl)phenyl)-2-((4-oxo-3-(4-methylphenyl)-3,4-dihydroquinazolin-2-yl)thio) acetamide 34_a

White crystals (yield 64 %); m.p.: 238-241°C; IR (KBr) cm^{-1}: 3250, 3117 (3NH), 1710, 1685 (3C=O), 1329, 1168 (SO_2).; ^{1}H NMR (DMSO.*d6*, δ ppm), 1.91 (s, 3H, $COCH_3$), 2.42 (s, 3H, C**H**$_3$-C_6H_5), 4.12 (s, 2H, S-CH_2), 7.35 (d, 2H, *J* = 6.5 Hz, Ar-H), 7.37 (d, 2H, *J* = 6.8 Hz, Ar-H), 7.44 (t, 1H, *J* = 6.8 Hz, Ar-H), 7.51 (d, 1H, *J* = 6.8 Hz, Ar-H), 7.77 (t, 1H, Ar-H), 7.82 (d, 2H, *J* = 7.6 Hz, Ar-H), 8.68 (d, 2H, *J* = 7.6 Hz, Ar-H), 8.07 (dd, 1H, *J* = 6.8, 7.6 Hz, Ar-H), 10.72 (s, 1H, CONH, D_2O exchangeable), 10.82 (s, 1H, -SO_2NH, D_2O exchangeable).; ^{13}C NMR; 21.34, 23.8, 119.04 (2C), 120.96, 124.36 (2C), 126.33, 127.09(2C), 129.39 (2C), 129.58 (2C), 130.52 (2C), 133.4, 135.38, 140.1, 144, 148, 158, 161, 168, 169. DEPT135 NMR; 21.34 (CH_3), 23.80 (CH_3), 37.77 (CH_2), 119.04 (2CH), 124.36, 126.33, 127.09, 129.39 (2CH), 129.58 (2CH), 130.52 (2CH), 135.38; Anal. Calcd. for $C_{25}H_{22}N_4O_5S_2$ (522.59): C, 57.46; H, 4.24; N, 10.72, Found: C, 57.70; H, 4.32; N, 10.89 %.

4.1.7.2. 2-((4-Oxo-3-(4-methylphenyl)-3,4-dihydroquinazolin-2-yl)thio)-N-(4-(N-(pyridin-2-yl)sulfamoyl) phenyl)acetamide 34_b

White crystals (yield 59 %); m.p.: 185-188 °C; IR (KBr) cm^{-1}: 3377, 3184 (2NH), 1685, 1671 (2C=O), 1316, 1149 (SO_2).; ^{1}H NMR (DMSO.*d6*, δ ppm): 2.41 (s, 3H, C**H**$_3$-C_6H_5), 4.09 (s, 2H, -SCH_2), 6.75 (d, 1H, *J* = 7.6 Hz, Ar-H), 7.13 (d, 1H, *J* = 8.0 Hz, Ar-H), 7.36 (d, 2H, *J* = 7.2 Hz, Ar-H), 7.44 (d, 2H, *J* = 7.2 Hz, Ar-H), 7.49 (d, 1H, *J* = 8.4 Hz, Ar-H), 7.63 (m, 2H, Ar-H), 7.7 (t, 1H, Ar-H), 7.74 (d, 2H, *J* = 8.8 Hz, Ar-H), 7.84 (d, 2H, *J* = 8.8 Hz, Ar-H), 8.0 (d, 1H, *J* = 6.4 Hz, Ar-H), 8.06 (d, 1H, *J* = 8.0 Hz, Ar-H), 10.71 (s, 1H, CONH, D_2O exchangeable), 10.86 (s, 1H, SO_2NH, D_2O exchangeable).; **^{13}C NMR**; 21.33, 37.75, 114.01, 116.15, 119.11 (2C), 119.98, 126.31, 126.46, 127.08, 127.41, 128.34 (2C), 129.57 (2C), 130.52 (2C), 133.59, 135.35, 136.44, 140.21, 140.55, 142.68, 147.54, 153.58, 157.60, 161.13, 166.98; DEPT135 NMR; 21.33 (1CH_3), 37.75 (1CH_2), 114, 119.09 (2CH), 126.31, 127.07, 127.40, 128.34 (2CH), 129.56 (2CH), 130.52 (2CH), 135.35, 140.54, 142.28, 142.65; Anal. Calcd. for $C_{28}H_{23}N_5O_4S_2$ (557.64): C, 60.31; H, 4.16; N, 12.56 Found: C, 60.48; H, 4.33; N, 12.81 %.

4.1.7.3. N-(4-(N-(4,6-Dimethylpyrimidin-2-yl)sulfamoyl)phenyl)-2-((4-oxo-3-(4-methylphenyl)-3,4-dihydro quinazolin-2-yl)thio)acetamide 34$_c$

Beige crystals (yield 60 %); m.p.: 241-243 ^{o}C; IR (KBr) cm^{-1}: 3447, 3189 (2NH), 1692 (2C=O), 1316, 1149 (SO_2).; ^{1}H NMR (DMSO.*d6*, δ ppm; 2.40 (s, 6H, 2CH_3), 2.51 (s, 3H, C**H$_3$** - C_6H_5), 4.09 (s, 2H, -SCH_2), 6.71 (s, 1H, Ar-H), 7.11 (d, 1H, *J* = 6.8 Hz, Ar-H), 7.33 (d, 2H, *J* = 6.8 Hz, Ar-H), 7.37 (d, 2H, *J* = 6.8 Hz, Ar-H), 7.42 (t, 1H, *J* = 6.8 Hz, Ar-H), 7.48 (d, 1H, *J* = 6.4 Hz, Ar-H), 7.76 (d, 2H, J = 6.4 Hz, Ar-H), 7.95 (d, 2H, *J* = 6.4 Hz, Ar-H), 8.05 (dd, 1H, *J* = 6.4, 6.0 Hz, ArH), 9.67 (s, 1H, CONH, D_2O exchangeable), 10.74 (s, 1H, SO_2NH, D_2O exchangeable); ^{13}C NMR; 21.32 (2C), 23.31, 37.73, 118.54 (2C), 119.97, 120.96, 124.34, 126.29, 126.46, 127.07, 129.31, 129.55 (2C), 129.84 (2C), 130.52 (2C), 133.57, 134.05, 135.31, 137.33, 140.20, 147.53, 157.60, 161.11, 167.03, 180.07; DEPT135 NMR; 21.32 (2CH_3), 23.31 (CH_3), 37.73 (CH_2), 118.54 (2CH), 124.34, 126.29, 127.07, 129.31 (2CH), 129.55 (2CH), 129.84 (2CH), 130.52, 135.31.; Mass (*m/z*): 586.75 (M^+, 23.01 %), 90.22 (100 %).; Anal. Calcd. for $C_{29}H_{26}N_6O_4S_2$ (586.69): C, 59.37; H, 4.47; N, 14.32 Found: C, 59.05; H, 4.60; N, 14.59 %.

4.2. Biological testing

4.2.1. *In vitro* anti-proliferative activity

All the final synthesized compounds were estimated for their *in vitro* anti-proliferative activities using standard MTT method, against a panel of three human tumor cell lines namely; HepG2, MCF-7 and HCT-116. The cell lines were obtained from ATCC (American Type Culture Collection) via the Holding company for biological products and vaccines (VACSERA) (Cairo, Egypt). The anti-proliferative activity was measured in a quantitative manner using MTT assay protocol as described by Borenfreund and Puerner [71-73] as follows:

Cell lines were cultured in RPMI-1640 medium with 10% fetal bovine serum. Antibiotics added were 100 unit/ml penicillin and 100µg/ml streptomycin at 37 ^{o}C in a 5% CO_2 incubator. The cell lines were seeded in a 96-well plate at a density of 1.0 x 104 cells / well at 37 ^{o}C for 48 h under 5% CO_2. After incubation, the cells were treated with different concentration of synthesized compounds and incubated for 24 h. After 24 h of drug treatment, 20 µl of MTT solution at 5mg/ml was added and incubated for 4 h. Dimethyl sulfoxide (DMSO) in volume of 100 µl was added into each well to dissolve the purple formazan formed. The colorimetric assay was estimated and recorded at absorbance of 570 nm using a plate reader (EXL 800, USA). The relative cell viability in percentage was calculated as (A570 of treated samples/A570 of untreated sample) X 100. The results of IC_{50} values were calculated using the GraphPad Prism version 7. Each reaction was

performed in duplicate, and at least three independent determinations of each IC_{50} were made. The *P* values were calculated using the GraphPad Prism version 7 using sorafenib as standard.

Results for IC_{50} values of the active compounds are summarized in **Table 1**.

4.2.2. *In vitro* VEGFR-2 kinase assay

Inhibitory activity of the selected compounds **12, 18, 16_e, 16_f, 26, 27_a, 27_b, 28, 30, 33_a** and **33_c** against VEGFR-2 was evaluated using Human VEGFR-2 ELISA kit (Enzyme-Linked Immunosorbent Assay). A specific antibody for VEGFR-2 was seeded on a 96-well plate and 100 µL of the standard solution or the tested compound was added, all were incubated at room temperature for 2.5 hours. Then washed, 100 µL of the prepared biotin antibody was added, then incubated at room temperature for additional 1 hour. Washed, 100 µL of streptavidin solution was added then incubated for 45 min. at room temperature. Washed again, 100 µL of TMB Substrate reagent was added and incubated for 30 min. at room temperature. 50 µL of the stop solution was added, then read at 450 nm immediately. The standard curve was drawn, concentrations on the X-axis and the absorbance on the Y-axis**.**

4.3. Molecular docking

VEGFR-2 crystal structure of was downloaded from the Protein Data Bank, http://www.rcsb.org/pdb (PDB ID: 2OH4, resolution: 2.05 Å) using Discovery Studio 2.5 software. Water molecules were removed from the downloaded protein. Alternate conformations and valence monitor options were used to correct crystallographic disorders and unfilled valence atoms. The energy of the 2OH4 protein was minimized using CHARMm and MMFF94 force fields for charge and partial charge, respectively. The active binding site of the protein was identified and prepared for docking. Structures of the designed compounds and reference ligand, sorafenib, were sketched using ChemBioDraw Ultra 14.0. Structures were saved in MDL-SD file format. Next, the SD file was opened followed by protonation of the 3D structures Then, and energy was minimized by applying CHARMm and MMFF94 force fields. Energy minimization was carried out as described in the Supporting Information. The structures were then prepared for docking by optimization of the parameters. Docking was carried out using CDOCKER-CHARMm-based technique in the interface of Accelry's Discovery Studio 2.5[78, 79] . A maximum of 10 conformers was measured for each molecule in the docking analysis. Subsequently, the docking scores (CDOCKER interaction energy) of the most ideal pose of each of the docked molecules with the amino acids at the VEGFR-2 binding pocket were recorded [80, 81].

Author contribution

Khaled. El-Adl: design, supervision and writing manuscript; Abdel-Ghany A. El-Helby: supervision; Rezk R. Ayyad: supervision; Hazem A. Mahdy: writing manuscript; Mohamed M.

Khalifa: molecular docking carrying out and writing manuscript; Hamdy A. Elnagar: chemical synthesis; Ahmed. B. M. Mehany: biological testing; Ahmed. M. Metwaly: data analysis; Mostafa. A. Elhendawy: data analysis; Mohamed. M. Radwan: data analysis; Mahmoud. A. ElSohly**:** data analysis; Ibrahim H. Eissa**:** design, supervision and writing manuscript.

References

[1] J. Folkman, Angiogenesis in cancer, vascular, rheumatoid and other disease, Nature medicine, 1 (1995) 27-30.

[2] R.S. Kerbel, Tumor angiogenesis: past, present and the near future, Carcinogenesis, 21 (2000) 505-515.

[3] Y. Yang, L. Shi, Y. Zhou, H.-Q. Li, Z.-W. Zhu, H.-L. Zhu, Design, synthesis and biological evaluation of quinoline amide derivatives as novel VEGFR-2 inhibitors, Bioorganic & medicinal chemistry letters, 20 (2010) 6653-6656.

[4] A. Garofalo, A. Farce, S.v. Ravez, A.l. Lemoine, P. Six, P. Chavatte, L. Goossens, P. Depreux, Synthesis and structure–activity relationships of (aryloxy) quinazoline ureas as novel, potent, and selective vascular endothelial growth factor receptor-2 inhibitors, Journal of medicinal chemistry, 55 (2012) 1189-1204.

[5] M. Behdani, S. Zeinali, H. Khanahmad, M. Karimipour, N. Asadzadeh, K. Azadmanesh, A. Khabiri, S. Schoonooghe, M.H. Anbouhi, G. Hassanzadeh-Ghassabeh, Generation and characterization of a functional Nanobody against the vascular endothelial growth factor receptor-2; angiogenesis cell receptor, Molecular immunology, 50 (2012) 35-41.

[6] M.A. El-Zahabi, H. Sakr, K. El-Adl, M. Zayed, A.S. Abdelraheem, S.I. Eissa, H. Elkady, I.H. Eissa, Design, synthesis, and biological evaluation of new challenging thalidomide analogs as potential anticancer immunomodulatory agents, Bioorganic Chemistry, (2020) 104218.

[7] H.A. Mahdy, M.K. Ibrahim, A.M. Metwaly, A. Belal, A.B. Mehany, K.M. El-Gamal, A. El-Sharkawy, M.A. Elhendawy, M.M. Radwan, M.A. Elsohly, Design, synthesis, molecular modeling, in vivo studies and anticancer evaluation of quinazolin-4 (3H)-one derivatives as potential VEGFR-2 inhibitors and apoptosis inducers, Bioorganic Chemistry, 94 (2020) 103422.

[8] H.-T. Zhong, Y.-Z. Yu, C. Velasco, Molecular insights probing Bismurrayaquinone A as an angiogenesis inhibitor via inhibition of VEGFR-2 Kinase domain, (2011).

[9] D. Kang, X. Pang, W. Lian, L. Xu, J. Wang, H. Jia, B. Zhang, A.-L. Liu, G.-H. Du, Discovery of VEGFR2 inhibitors by integrating naïve Bayesian classification, molecular docking and drug screening approaches, RSC advances, 8 (2018) 5286-5297.

[10] M.A. Abdullaziz, H.T. Abdel-Mohsen, A.M. El Kerdawy, F.A. Ragab, M.M. Ali, S.M. Abu-bakr, A.S. Girgis, H.I. El Diwani, Design, synthesis, molecular docking and cytotoxic evaluation of novel 2-furybenzimidazoles as VEGFR-2 inhibitors, European journal of medicinal chemistry, 136 (2017) 315-329.

[11] A.G.A. El-Helby, H. Sakr, I.H. Eissa, A.A. Al-Karmalawy, K. El-Adl, Benzoxazole/benzothiazole-derived VEGFR-2 inhibitors: Design, synthesis, molecular docking, and anticancer evaluations, Archiv der Pharmazie, 352 (2019) 1900178.

[12] W.M. Eldehna, A.M. El Kerdawy, G.H. Al-Ansary, S.T. Al-Rashood, M.M. Ali, A.E. Mahmoud, Type IIA-Type IIB protein tyrosine kinase inhibitors hybridization as an efficient approach for potent multikinase inhibitor development: Design, synthesis, anti-proliferative activity, multikinase inhibitory activity and molecular modeling of novel indolinone-based ureides and amides, European journal of medicinal chemistry, 163 (2019) 37-53.

[13] C. Wang, J. Dong, Y. Zhang, F. Wang, H. Gao, P. Li, S. Wang, J. Zhang, Design, synthesis and biological evaluation of biphenyl urea derivatives as novel VEGFR-2 inhibitors, MedChemComm, 4 (2013) 1434-1438.

[14] L. Lintnerová, M. García-Caballero, F. Gregáň, M. Melicherčík, A.R. Quesada, J. Dobiaš, J. Lác, M. Sališová, A. Boháč, A development of chimeric VEGFR2 TK inhibitor based on two ligand conformers from PDB: 1Y6A complex–Medicinal chemistry consequences of a TKs analysis, European journal of medicinal chemistry, 72 (2014) 146-159.

[15] M. Momeny, Z. Sabourinejad, G. Zarrinrad, F. Moghaddaskho, H. Eyvani, H. Yousefi, S. Mirshahvaladi, E.M. Poursani, F. Barghi, A. Poursheikhani, Anti-tumour activity of tivozanib, a pan-inhibitor of VEGF receptors, in therapy-resistant ovarian carcinoma cells, Scientific reports, 7 (2017) 1-13.

[16] S. Huang, R. Li, P.J. Connolly, G. Xu, M.D. Gaul, S.L. Emanuel, K.R. LaMontagne, L.M. Greenberger, Synthesis and biological study of 4-aminopyrimidine-5-carboxaldehyde oximes as antiproliferative VEGFR-2 inhibitors, Bioorganic & medicinal chemistry letters, 16 (2006) 6063-6066.

[17] Y. Luo, F. Jiang, T.B. Cole, V.P. Hradil, D. Reuter, A. Chakravartty, D.H. Albert, S.K. Davidsen, B.F. Cox, E.M. McKeegan, A novel multi-targeted tyrosine kinase inhibitor, linifanib (ABT-869), produces functional and structural changes in tumor vasculature in an orthotopic rat glioma model, Cancer chemotherapy and pharmacology, 69 (2012) 911-921.

[18] S.J. Klempner, A.P. Myers, G.B. Mills, S.N. Westin, Clinical investigation of receptor and non-receptor tyrosine kinase inhibitors for the treatment of epithelial ovarian cancer, Expert opinion on pharmacotherapy, 14 (2013) 2171-2182.

[19] I. Ruscito, M.L. Gasparri, C. Marchetti, C. De Medici, C. Bracchi, I. Palaia, S. Imboden, M.D. Mueller, A. Papadia, L. Muzii, Cediranib in ovarian cancer: state of the art and future perspectives, Tumor biology, 37 (2016) 2833-2839.

[20] M. Li, X. Yu, W. Li, T. Liu, G. Deng, W. Liu, H. Liu, F. Gao, Deguelin suppresses angiogenesis in human hepatocellular carcinoma by targeting HGF-c-Met pathway, Oncotarget, 9 (2018) 152.

[21] H. Wang, B. Rao, J. Lou, J. Li, Z. Liu, A. Li, G. Cui, Z. Ren, Z. Yu, The Function of the HGF/c-Met Axis in Hepatocellular Carcinoma, Frontiers in Cell and Developmental Biology, 8 (2020) 55.

[22] L. Goyal, M.D. Muzumdar, A.X. Zhu, Targeting the HGF/c-MET pathway in hepatocellular carcinoma, Clinical Cancer Research, 19 (2013) 2310-2318.

[23] Y. Zhang, X. Gao, Y. Zhu, D. Kadel, H. Sun, J. Chen, Q. Luo, H. Sun, L. Yang, J. Yang, The dual blockade of MET and VEGFR2 signaling demonstrates pronounced inhibition on tumor growth and metastasis of hepatocellular carcinoma, Journal of Experimental & Clinical Cancer Research, 37 (2018) 1-15.

[24] Z. Liu, L. Qi, Y. Li, X. Zhao, B. Sun, VEGFR2 regulates endothelial differentiation of colon cancer cells, BMC cancer, 17 (2017) 593.

[25] M. Zhong, N. Li, X. Qiu, Y. Ye, H. Chen, J. Hua, P. Yin, G. Zhuang, TIPE regulates VEGFR2 expression and promotes angiogenesis in colorectal cancer, International journal of biological sciences, 16 (2020) 272.

[26] R. Aesoy, B.C. Sanchez, J.H. Norum, R. Lewensohn, K. Viktorsson, B. Linderholm, An autocrine VEGF/VEGFR2 and p38 signaling loop confers resistance to 4-hydroxytamoxifen in MCF-7 breast cancer cells, Molecular Cancer Research, 6 (2008) 1630-1638.

[27] K. van Rossem, J.A. Lowe, A Phase 1, randomized, open-label crossover study to evaluate the safety and pharmacokinetics of 400 mg albaconazole administered to healthy participants as a tablet formulation versus a capsule formulation, Clinical pharmacology: advances and applications, 5 (2013) 23.

[28] S.E. Abbas, F.F. Barsoum, H.H. Georgey, E.R. Mohammed, Synthesis and antitumor activity of certain 2, 3, 6-trisubstituted quinazolin-4 (3H)-one derivatives, Bulletin of Faculty of Pharmacy, Cairo University, 51 (2013) 273-282.

[29] M. Kumar, B. Narasimhan, P. Kumar, K. Ramasamy, V. Mani, R.K. Mishra, A.B.A. Majeed, 4-(1-Aryl-5-chloro-2-oxo-1, 2-dihydro-indol-3-ylideneamino)-N-substituted benzene sulfonamides: Synthesis, antimicrobial, anticancer evaluation and QSAR studies, Arabian Journal of Chemistry, 7 (2014) 436-447.

[30] I.H. Eissa, A.-G.A. El-Helby, H.A. Mahdy, M.M. Khalifa, H.A. Elnagar, A.B. Mehany, A.M. Metwaly, M.A. Elhendawy, M.M. Radwan, M.A. ElSohly, Discovery of new quinazolin-4 (3H)-ones

as VEGFR-2 inhibitors: Design, synthesis, and anti-proliferative evaluation, Bioorganic Chemistry, (2020) 104380.

[31] M.L. de Castro Barbosa, L.M. Lima, R. Tesch, C.M.R. Sant'Anna, F. Totzke, M.H. Kubbutat, C. Schächtele, S.A. Laufer, E.J. Barreiro, Novel 2-chloro-4-anilino-quinazoline derivatives as EGFR and VEGFR-2 dual inhibitors, European journal of medicinal chemistry, 71 (2014) 1-14.

[32] W.-x. Hu, W. Zhou, C.-n. Xia, X. Wen, Synthesis and anticancer activity of thiosemicarbazones, Bioorganic & medicinal chemistry letters, 16 (2006) 2213-2218.

[33] M. Ibrahim, M. Taghour, A.M. Metwaly, A. Belal, A. Mehany, M. Elhendawy, M. Radwan, A. Yassin, N. El-Deeb, E. Hafez, Design, synthesis, molecular modeling and anti-proliferative evaluation of novel quinoxaline derivatives as potential DNA intercalators and topoisomerase II inhibitors, European journal of medicinal chemistry, 155 (2018) 117-134.

[34] A.A. Gaber, A.H. Bayoumi, A.M. El-morsy, F.F. Sherbiny, A.B. Mehany, I.H. Eissa, Design, synthesis and anticancer evaluation of 1H-pyrazolo [3, 4-d] pyrimidine derivatives as potent EGFRWT and EGFRT790M inhibitors and apoptosis inducers, Bioorganic Chemistry, 80 (2018) 375-395.

[35] I.H. Eissa, A.M. El-Naggar, N.E. El-Sattar, A.S. Youssef, Design and discovery of novel quinoxaline derivatives as dual DNA intercalators and topoisomerase II inhibitors, Anti-Cancer Agents in Medicinal Chemistry (Formerly Current Medicinal Chemistry-Anti-Cancer Agents), 18 (2018) 195-209.

[36] A.M. El-Naggar, M.M. Abou-El-Regal, S.A. El-Metwally, F.F. Sherbiny, I.H. Eissa, Synthesis, characterization and molecular docking studies of thiouracil derivatives as potent thymidylate synthase inhibitors and potential anticancer agents, Molecular diversity, 21 (2017) 967-983.

[37] W.M. Eldehna, M.F. Abo-Ashour, A. Nocentini, P. Gratteri, I.H. Eissa, M. Fares, O.E. Ismael, H.A. Ghabbour, M.M. Elaasser, H.A. Abdel-Aziz, Novel 4/3-((4-oxo-5-(2-oxoindolin-3-ylidene) thiazolidin-2-ylidene) amino) benzenesulfonamides: synthesis, carbonic anhydrase inhibitory activity, anticancer activity and molecular modelling studies, European journal of medicinal chemistry, 139 (2017) 250-262.

[38] I.H. Eissa, A.M. El-Naggar, M.A. El-Hashash, Design, synthesis, molecular modeling and biological evaluation of novel 1H-pyrazolo [3, 4-b] pyridine derivatives as potential anticancer agents, Bioorganic Chemistry, 67 (2016) 43-56.

[39] S.A. Elmetwally, K.F. Saied, I.H. Eissa, E.B. Elkaeed, Design, synthesis and anticancer evaluation of thieno [2, 3-d] pyrimidine derivatives as dual EGFR/HER2 inhibitors and apoptosis inducers, Bioorganic Chemistry, 88 (2019) 102944.

[40] I.H. Eissa, A.M. Metwaly, A. Belal, A.B. Mehany, R.R. Ayyad, K. El-Adl, H.A. Mahdy, M.S. Taghour, K.M. El-Gamal, M.E. El-Sawah, Discovery and antiproliferative evaluation of new quinoxalines as potential DNA intercalators and topoisomerase II inhibitors, Archiv der Pharmazie, 352 (2019) 1900123.

[41] A.G.A. El-Helby, H. Sakr, I.H. Eissa, H. Abulkhair, A.A. Al-Karmalawy, K. El-Adl, Design, synthesis, molecular docking, and anticancer activity of benzoxazole derivatives as VEGFR-2 inhibitors, Archiv der Pharmazie, 352 (2019) 1900113.

[42] A.-G.A. El-Helby, H. Sakr, R.R. Ayyad, K. El-Adl, M.M. Ali, F. Khedr, Design, Synthesis, In Vitro Anti-cancer Activity, ADMET Profile and Molecular Docking of Novel Triazolo [3, 4-a] phthalazine Derivatives Targeting VEGFR-2 Enzyme, Anti-Cancer Agents in Medicinal Chemistry (Formerly Current Medicinal Chemistry-Anti-Cancer Agents), 18 (2018) 1184-1196.

[43] A.G.A. El-Helby, R.R. Ayyad, H. Sakr, K. El-Adl, M.M. Ali, F. Khedr, Design, Synthesis, Molecular Docking, and Anticancer Activity of Phthalazine Derivatives as VEGFR-2 Inhibitors, Archiv der Pharmazie, 350 (2017) 1700240.

[44] A.M. El-Naggar, I.H. Eissa, A. Belal, A.A. El-Sayed, Design, eco-friendly synthesis, molecular modeling and anticancer evaluation of thiazol-5 (4 H)-ones as potential tubulin polymerization inhibitors targeting the colchicine binding site, RSC Advances, 10 (2020) 2791-2811.

[45] K. El-Adl, A.-G.A. El-Helby, H. Sakr, I.H. Eissa, S.S. El-Hddad, F.M. Shoman, Design, synthesis, molecular docking and anticancer evaluations of 5-benzylidenethiazolidine-2, 4-dione derivatives targeting VEGFR-2 enzyme, Bioorganic Chemistry, 102 (2020) 104059.

[46] A.-G.A. El-Helby, H. Sakr, R.R. Ayyad, H.A. Mahdy, M.M. Khalifa, A. Belal, M. Rashed, A. El-Sharkawy, A.M. Metwaly, M.A. Elhendawy, Design, synthesis, molecular modeling, in vivo studies and anticancer activity evaluation of new phthalazine derivatives as potential DNA intercalators and topoisomerase II inhibitors, Bioorganic Chemistry, (2020) 104233.

[47] Q.-Q. Xie, H.-Z. Xie, J.-X. Ren, L.-L. Li, S.-Y. Yang, Pharmacophore modeling studies of type I and type II kinase inhibitors of Tie2, Journal of Molecular Graphics and Modelling, 27 (2009) 751-758.

[48] K. Lee, K.-W. Jeong, Y. Lee, J.Y. Song, M.S. Kim, G.S. Lee, Y. Kim, Pharmacophore modeling and virtual screening studies for new VEGFR-2 kinase inhibitors, European journal of medicinal chemistry, 45 (2010) 5420-5427.

[49] R.N. Eskander, K.S. Tewari, Incorporation of anti-angiogenesis therapy in the management of advanced ovarian carcinoma—mechanistics, review of phase III randomized clinical trials, and regulatory implications, Gynecologic oncology, 132 (2014) 496-505.

[50] V.A. Machado, D. Peixoto, R. Costa, H.J. Froufe, R.C. Calhelha, R.M. Abreu, I.C. Ferreira, R. Soares, M.-J.R. Queiroz, Synthesis, antiangiogenesis evaluation and molecular docking studies of 1-aryl-3-[(thieno [3, 2-b] pyridin-7-ylthio) phenyl] ureas: Discovery of a new substitution pattern for type II VEGFR-2 Tyr kinase inhibitors, Bioorganic & medicinal chemistry, 23 (2015) 6497-6509.
[51] Z. Wang, N. Wang, S. Han, D. Wang, S. Mo, L. Yu, H. Huang, K. Tsui, J. Shen, J. Chen, Dietary compound isoliquiritigenin inhibits breast cancer neoangiogenesis via VEGF/VEGFR-2 signaling pathway, PloS one, 8 (2013).
[52] A. Garofalo, L. Goossens, P. Six, A. Lemoine, S. Ravez, A. Farce, P. Depreux, Impact of aryloxy-linked quinazolines: A novel series of selective VEGFR-2 receptor tyrosine kinase inhibitors, Bioorganic & medicinal chemistry letters, 21 (2011) 2106-2112.
[53] M.A. Aziz, R.A. Serya, D.S. Lasheen, A.K. Abdel-Aziz, A. Esmat, A.M. Mansour, A.N.B. Singab, K.A. Abouzid, Discovery of potent VEGFR-2 inhibitors based on furopyrimidine and thienopyrimidne scaffolds as cancer targeting agents, Scientific reports, 6 (2016) 24460.
[54] G.A. El-Hiti, M.F. Abdel-Megeed, T.M. Zied, Synthesis and reactions of some 3-aryl-2-thioxoquinazolin-4 (3H)-ones, (2002).
[55] M.K. Ibrahim, I.H. Eissa, A.E. Abdallah, A.M. Metwaly, M. Radwan, M. ElSohly, Design, synthesis, molecular modeling and anti-hyperglycemic evaluation of novel quinoxaline derivatives as potential PPARγ and SUR agonists, Bioorganic & medicinal chemistry, 25 (2017) 1496-1513.
[56] J. Maru, G. PATEL, R. YADAV, B. BHATT, Synthesis and study of some novel benzothiazole derivatives as antimicrobial agents, J. Curr. Chem. Pharm. Sc, 4 (2014) 164-171.
[57] A.G.A. El-Helby, R.R. Ayyad, H.M. Sakr, A.S. Abdelrahim, K. El-Adl, F.S. Sherbiny, I.H. Eissa, M.M. Khalifa, Design, synthesis, molecular modeling and biological evaluation of novel 2, 3-dihydrophthalazine-1, 4-dione derivatives as potential anticonvulsant agents, Journal of Molecular Structure, 1130 (2017) 333-351.
[58] B.S. Furniss, Vogel's textbook of practical organic chemistry, Pearson Education India, 1989.
[59] J.R. Maxwell, D.A. Wasdahl, A.C. Wolfson, V.I. Stenberg, Synthesis of 5-aryl-2H-tetrazoles, 5-aryl-2H-tetrazole-2-acetic acids, and [(4-phenyl-5-aryl-4H-1, 2, 4-triazol-3-yl) thio] acetic acids as possible superoxide scavengers and antiinflammatory agents, Journal of medicinal chemistry, 27 (1984) 1565-1570.
[60] K. Sung, A.R. Lee, Synthesis of [(4, 5-disubstituted-4H-1, 2, 4-triazol-3-yl) thio] alkanoic acids and their analogues as possible antiinflammatory agents, Journal of heterocyclic chemistry, 29 (1992) 1101-1109.

[61] M. Salem, H. Thabet, M. Helal, A. Abdelaal, Y. Ammar, Synthesis and pharmacological evaluation of some pyrazoles, thiazolopyrimidine, triazolopyrimidine, pyridone and 2-iminochromene containing naproxenoyl moiety as NSAIDs, Chemical Sciences Journal, (2011).

[62] W.A. Jacobs, M. Heidelberger, METHODS FOR THE ACYLATION OF AROMATIC AMINO COMPOUNDS AND UREAS, WITH ESPECIAL REFERENCE TO CHLOROACETYLATION, Journal of the American Chemical Society, 39 (1917) 1439-1447.

[63] F.M. Chen, N.L. Benoiton, The preparation and reactions of mixed anhydrides of N-alkoxycarbonylamino acids, Canadian journal of chemistry, 65 (1987) 619-625.

[64] D. Hangauer, M. Al-Zahaby, Methodology for preparing combinatorial libraries based upon a bicyclic scaffold, in, Google Patents, 2005.

[65] M. Alswah, A. Ghiaty, A. El-Morsy, K. El-Gamal, Synthesis and biological evaluation of some [1, 2, 4] triazolo [4, 3-a] quinoxaline derivatives as novel anticonvulsant agents, ISRN organic chemistry, 2013 (2013).

[66] J. Finkelstein, N4-Substituted Sulfonamides, Journal of the American Chemical Society, 66 (1944) 407-408.

[67] A.A. Farag, S.N. Abd-Alrahman, G.F. Ahmed, R.M. Ammar, Y.A. Ammar, S.Y. Abbas, Synthesis of some azoles incorporating a sulfonamide moiety as anticonvulsant agents, Archiv der Pharmazie, 345 (2012) 703-712.

[68] J.-C. Lee, N.-H. Chow, S.-T. Wang, S.-M. Huang, Prognostic value of vascular endothelial growth factor expression in colorectal cancer patients, European Journal of Cancer, 36 (2000) 748-753.

[69] L. Hlatky, C. Tsionou, P. Hahnfeldt, C.N. Coleman, Mammary fibroblasts may influence breast tumor angiogenesis via hypoxia-induced vascular endothelial growth factor up-regulation and protein expression, Cancer research, 54 (1994) 6083-6086.

[70] R.T.-P. Poon, C.P.-Y. Lau, S.-T. Cheung, W.-C. Yu, S.-T. Fan, Quantitative correlation of serum levels and tumor expression of vascular endothelial growth factor in patients with hepatocellular carcinoma, Cancer research, 63 (2003) 3121-3126.

[71] T. Mosmann, Rapid colorimetric assay for cellular growth and survival: application to proliferation and cytotoxicity assays, Journal of immunological methods, 65 (1983) 55-63.

[72] F. Denizot, R. Lang, Rapid colorimetric assay for cell growth and survival: modifications to the tetrazolium dye procedure giving improved sensitivity and reliability, Journal of immunological methods, 89 (1986) 271-277.

[73] M.I. Thabrew, R.D. HUGHES, I.G. MCFARLANE, Screening of hepatoprotective plant components using a HepG2 cell cytotoxicity assay, Journal of pharmacy and pharmacology, 49 (1997) 1132-1135.

[74] Y. Liu, N.S. Gray, Rational design of inhibitors that bind to inactive kinase conformations, Nature chemical biology, 2 (2006) 358-364.

[75] A. Monirah, A. Danah, E. Fatima, Synthesis of some-2-thioxo-3-substituted-2, 3-dihydro-1H-quinazolin-4-one derivatives as potential antibacterial and antifungal agents, Res J Chem Environ, 17 (2013) 48-52.

[76] M.G. Al-Khuzaie, S.M. Al-Majidi, Synthesis, characterization and evaluation antimicrobial activity of some new substituted 2-mercapto-3-phenyl-4 (3H)-quinazolinone, Iraqi Journal of Science, 55 (2014) 582-593.

[77] A.A. Kanhed, A.P. Mehere, K.R. Pandey, D.K. Mahapatra, 4-(2-chloroacetamido) Benzoic acid derivatives as local anesthetic agents: design, synthesis, and characterization, UK J Pharm Biosci, 4 (2016) 35-44.

[78] M.K. Ibrahim, I.H. Eissa, M.S. Alesawy, A.M. Metwaly, M.M. Radwan, M.A. ElSohly, Design, synthesis, molecular modeling and anti-hyperglycemic evaluation of quinazolin-4 (3H)-one derivatives as potential PPARγ and SUR agonists, Bioorganic & medicinal chemistry, 25 (2017) 4723-4744.

[79] M.A. El-Zahabi, E.R. Elbendary, F.H. Bamanie, M.F. Radwan, S.A. Ghareib, I.H. Eissa, Design, synthesis, molecular modeling and anti-hyperglycemic evaluation of phthalimide-sulfonylurea hybrids as PPARγ and SUR agonists, Bioorganic chemistry, 91 (2019) 103115.

[80] E.M. Abbass, A.K. Khalil, M.M. Mohamed, I.H. Eissa, A.M. El-Naggar, Design, efficient synthesis, docking studies, and anticancer evaluation of new quinoxalines as potential intercalative Topo II inhibitors and apoptosis inducers, Bioorganic Chemistry, (2020) 104255.

[81] I. Eissa, H. Mahdy, A. Mehany, M. Taghour, A. Belal, M. El-Zahabi, A. Nasser, A.M. Saleh, W. Afifi, H. Luesch, Discovery of new pyrimidine-5-carbonitrile derivatives as anticancer agents targeting EGFRWT and EGFRT790M, Organic & Biomolecular Chemistry, (2020).

Highlights

- Nineteen compounds of novel quinazolin-4(3*H*)-one derivatives were designed and synthesized.
- Cytotoxic activities were evaluated against HepG-2, MCF-7 and HCT-116 cell lines
- *In vitro* anti VEGFR-2 activities were evaluated.
- Molecular docking studies were carried out.

Graphical abstract

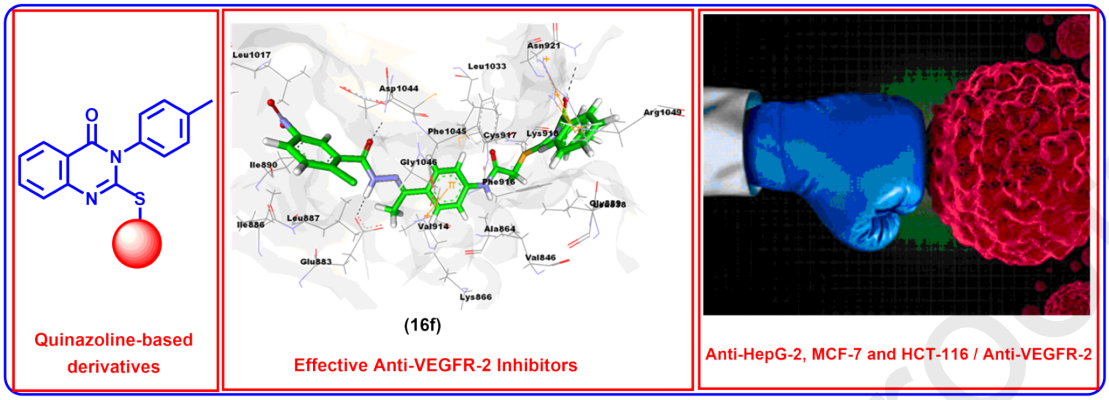

AUTHOR DECLARATION

We wish to confirm that there are no known conflicts of interest associated with this publication and there has been no significant financial support for this work that could have influenced its outcome.

We confirm that the manuscript has been read and approved by all named authors and that there are no other persons who satisfied the criteria for authorship but are not listed. We further confirm that the order of authors listed in the manuscript has been approved by all of us.

We confirm that we have given due consideration to the protection of intellectual property associated with this work and that there are no impediments to publication, including the timing of publication, with respect to intellectual property. In so doing we confirm that we have followed the regulations of our institutions concerning intellectual property.

We further confirm that any aspect of the work covered in this manuscript that has involved experimental animals has been conducted with the ethical approval of all relevant bodies.

We understand that the Corresponding Author is the sole contact for the Editorial process. He is responsible for communicating with the other authors about progress, submissions of revisions and final approval of proofs. We confirm that we have provided a current, correct email address which is accessible by the Corresponding Author and which has been configured to accept email from : Ibrahimeissa@azhar.edu.eg

Khaled EL-Adl: eladlkhaled74@yahoo.com
Abdel-Ghany A. El-Helby easa1979@yahoo.com
Mohamed M. Khalifa: khalifa_mohamed22@yahoo.com
Hamdy A. Elnagar: hamdy_pharm@yahoo.com
Ahmed M. Metwaly ametwaly@azhar.edu.eg
Ahmed B. M. Mehany: abelal_81@yahoo.com
Mahmoud A. ElSohly msohly@olemiss.edu
Mohamed M. Radwan mradwan@olemiss.edu

Mostafa A. Elhendawy elhendawy3000@yahoo.com